



Spatial Patterns of Microplastics in Surface Seawater, Sediment, and Sand Along Qingdao Coastal Environment

Yadan Luo¹, Cuizhu Sun¹, Chenguang Li¹, Yifan Liu¹, Shasha Zhao¹, Yuanyuan Li¹, Fanna Kong^{2,3*}, Hao Zheng^{1,4*}, Xianxiang Luo^{1,4}, Lingyun Chen⁵ and Fengmin Li^{1,4}

OPEN ACCESS

Edited by:

Qing Wang,
Yantai Institute of Coastal Zone
Research (CAS), China

Reviewed by:

Bijuan Chen,
Chinese Academy of Fishery Sciences
(CAFS), China
Abolfazl Naji,
Leibniz Centre for Tropical Marine
Research (LG), Germany

*Correspondence:

Fanna Kong
finkong@ouc.edu.cn
Hao Zheng
zhenghao2013@ouc.edu.cn

Specialty section:

This article was submitted to
Marine Pollution,
a section of the journal
Frontiers in Marine Science

Received: 10 April 2022

Accepted: 25 April 2022

Published: 26 May 2022

Citation:

Luo Y, Sun C, Li C, Liu Y, Zhao S,
Li Y, Kong F, Zheng H, Luo X, Chen L
and Li F (2022) Spatial Patterns of
Microplastics in Surface Seawater,
Sediment, and Sand Along
Qingdao Coastal Environment.
Front. Mar. Sci. 9:916859.
doi: 10.3389/fmars.2022.916859

¹ Key Laboratory of Marine Environment and Ecology, Institute of Coastal Environmental Pollution Control, College of Environmental Science and Engineering, Ministry of Education, Frontiers Science Center for Deep Ocean Multispheres and Earth System, Ocean University of China, Qingdao, China, ² Key Laboratory of Marine Genetics and Breeding, Ministry of Education, College of Marine Life Sciences, Ocean University of China, Qingdao, China, ³ College of Marine Life Sciences, Ocean University of China, Qingdao, China, ⁴ Marine Ecology and Environmental Science Laboratory, Pilot National Laboratory for Marine Science and Technology, Qingdao, China, ⁵ Faculty of Agricultural, Life and Environmental Science, University of Alberta, Edmonton, AB, Canada

Coastal environments, ecologically fragile zones, are subjected to great human pressures, particularly, xenobiotic pollutants such as microplastics (MPs) and trace metals. Yet, the impact of anthropogenic intervention on the spatial patterns of MPs in different coastal environmental compartments of Qingdao, a city located in the west Yellow Sea, is still unclear. Therefore, the spatial distribution, characteristics, and diversity of MPs ($\geq 50 \mu\text{m}$) in seawater, sediment, and sand samples collected from 10 zones intervened by different anthropogenic activities in Qingdao coastal environment were investigated. The abundance of MPs was 93.1 ± 63.5 items/ m^3 in seawater, which was 4577 ± 2902 items/kg in sediments and 3602 ± 1708 items/kg in the beach sands. A spatial analysis indicated that the distribution characteristics of MPs, including abundance, color, and type, greatly varied among the zones with different extent of human activities. The highest abundance of MPs in the seawater was detected in the abandoned aquafarm, followed by harbors, beaches, estuary, sewage discharge areas, operational aquafarm, and rural areas, whereas the highest MP abundance in the sediments followed the order of harbor, sewage discharge, estuary, abandoned aquafarm, beaches, rural area, and operational aquafarm. The highest MP abundance in the scenic and recreational beach sands was, respectively, in the intertidal and supratidal zone. The transparent chlorinated polyethylene fragments with the relatively small size of 50–100 μm were the dominant MPs in the coastal environment. The higher physicochemical characteristic diversity in terms of size, color, shape, and type of MPs in the aquafarms, harbors, and recreational beach than those of the other zones, illustrated the higher complexity and diversity of MP pollution

sources in these zones. These results jointly indicated that aquaculture, navigation, and tourism mainly determined MP spatial distribution patterns in the coastal environment of Qingdao. These results also extend the understanding of the inventory and fate of MPs in coastal environment, thus providing important data to establish effective strategies for abating MP pollution in marine ecosystems.

Keywords: coastal environment, anthropogenic activities, microplastic diversity, aquafarm, spatial distribution

INTRODUCTION

Wide application of plastic products in various fields such as packaging, construction, automobile manufacturing, agriculture, and medical has resulted in a large amount of plastic production (Meng et al., 2020). The annual production output of plastics has grown from 1.5 million metric tons (Mt) in 1950 to 367 million Mt in 2020 (Plastics Europe, 2021). However, approximately 79% of global plastic wastes entered into landfills or directly discarded into natural environment (Geyer et al., 2017) because of poor waste management and low capacity to dispose of or recycle waste plastics (Jambeck et al., 2015). Once entering into the marine environment, large plastic debris could be degraded into smaller particles such as microplastics (< 5 mm, MPs) (Li et al., 2019), and even nanoplastics (< 100 nm, NPs) (Hartmann et al., 2019), by weathering (e.g., abrasion, fluctuation, and turbulence), ultraviolet radiation, and microbial degradation (Dong et al., 2020). An estimation reported that ~8 million Mt macroplastic (≥ 5 mm) and 1.5 Mt primary MPs (micron particles from personal care products and product ingredients in factories) entered ocean annually (Lau et al., 2020). Extensive studies reported that MPs have been detected in a variety of marine ecosystems, from equator to poles (Cózar et al., 2014), from surface water to hadal sediment (Peng et al., 2020), and from coast to open sea (Chae and An, 2017). Because of the small size, strong adsorption affinity, and high persistence, MPs are highly bioavailable to marine organisms at different trophic levels through direct ingestion or indirect trophic transfer (Peng et al., 2020; Santos et al., 2021). MPs can be ingested and accumulated by marine organisms, such as phytoplankton (Peller et al., 2021), zooplankton (Liu L., et al., 2021; Wang et al., 2020a), macroalgae (Zhang et al., 2022), fish (Wang et al., 2020a), and marine mammals (Nelms et al., 2019). Once ingested, MPs can pose adverse effects on the digestive glands (Kang et al., 2020; Trestrail et al., 2021), reproduction (Duan et al., 2020), and immune and nervous systems (Liu Y. et al., 2021), thus resulting in reduction in ingestion (Oliveira et al., 2021) and energy reserves (Gardona et al., 2020). Furthermore, MPs could serve as vectors to transport/co-transport hazardous substances (e.g., persistent organic pollutants, trace metals, and pathogens) because of the strong sorption affinity, thus potentially leading to combined toxicity (Akhbarizadeh et al., 2018). Moreover, the accumulation of MPs in water and sediment may affect nitrogen cycling (e.g., inhibited nitrification and denitrification) and C cycling (e.g., restricted marine carbon pump due to variation of the biofilms on MPs) (MacLeod et al., 2021). Occurrence of MPs, as novel substrates for biofilm formation in a natural

environment (Chen et al., 2020), also could alter microbial community composition and function (Xie et al., 2021) and promote spread and diffusion of antibiotic resistance genes (Wang et al., 2019). Therefore, the pollution of MPs has become a growing concern in global environmental issues and should be roundly monitored.

Coastal environments, including mangroves, salt marshes, coral reefs, beaches, and dunes, the pivotal links between terrestrial and oceanic ecosystems (Pintado-Herrera et al., 2020), carry many crucial functions including habitat creation for species (Tu et al., 2020), biogeochemical processing (Lastra et al., 2015), and regulating global climate (Gaylard et al., 2020). Also, coastal ecosystems could provide important services for humans such as international trade, recreational activities, and cultural services (Zheng et al., 2020). Coastal environments, the typical ecotones with high sensitivity and fragile features (Fu et al., 2021), have been subjected by heavy burdens of anthropic stressors. Nearly 60% of the population in the world live in global coastal environments (Zheng et al., 2020), leading to the loss of habitat and degradation of biodiversity in the coastal environments, particularly, the increasing inputs of exogenous pollutants into coastal environments due to the rapid development of urbanization and industrialization, including polycyclic aromatic hydrocarbons, polychlorinated biphenyls, organochlorine pesticides (Jebara et al., 2020), trace metals (Bai et al., 2022), pharmaceutical and personal care products (PPCPs) (Sadutto et al., 2021), engineered nanoparticles (Li et al., 2018), and plastic wastes (Sun et al., 2020). Among them, plastic wastes, particularly MPs, have attracted increasing attention due to their small size, persistence, and toxicity (Patchaiyappan et al., 2021). Increasing studies showed that MP pollution in coastal environments greatly varied with geographic locations (Brignac et al., 2019; Liu L., et al., 2021). For example, the MP abundance detected in the Yellow Sea were 0.1–0.5 items/m³ in seawater (Wang et al., 2018) and 72.0–124 items/kg in sediment (Zhao J. et al., 2018), but the abundance in the Baltic Sea was 200–1388 items/m³ in seawater and 63.4–106 items/kg in sediment (Bagaev et al., 2018; Hengstmann et al., 2018). These studies demonstrated that anthropogenic activities such as aquaculture, navigation, and tourism greatly influenced the MP distribution in coastal environments (Xue et al., 2020; Dibke et al., 2021; Chen L., et al., 2021). However, inconsistent results were also reported. Zhu et al. (2019) found that MP abundance in the Maowei Sea was comparable to that in inflowing rivers, but Li et al. (2019) detected that MPs in the estuary of the Maowei Sea were much lower than those at the oceanic entrance zones. These distinct results are mainly ascribed to the geographic conditions

(e.g., hydrological conditions, environmental media heterogeneity) (Brignac et al., 2019; Liu Y. et al., 2021), and human activities (e.g., aquaculture, navigation, sewage discharge from wastewater treatment plants (WWTPs), and waste discarded by tourists) (Dowarah and Devipriya, 2019; Park et al., 2020; Sui et al., 2020; Zhou et al., 2020; Dibke et al., 2021; Chen C. F., et al., 2021). In addition, natural factors such as monsoon (Xu et al., 2022), heavy rainfall (Liu et al., 2020), typhoon (Chen L., et al., 2021), and season (Chen L., et al., 2021) also increased the abundance of MPs in coastal environments. The coastal environment is a complicated ecosystem, therefore, the distribution of MPs was often influenced by a combination of several factors. Moreover, besides the natural conditions and human activities, these variations in MP distribution in coastal environments were also attributed to the differences in sampling, extraction, and detection methods for qualitative and quantitative analysis of MPs (Prata et al., 2019, which was due to lack of international standards. Most of these investigations mainly focused on the MPs with relatively larger size ($\geq 330 \mu\text{m}$) by trawling methods (Brignac et al., 2019; Lenaker et al., 2019; Prata et al., 2019). Hence, they overlooked the MPs with smaller size ($< 330 \mu\text{m}$), particularly the size of $50\text{--}200 \mu\text{m}$, which were closer to the size of algae and were easily ingested by organisms (Lindeque et al., 2020). Obviously, these findings illustrate the complexities and uncertainties of MP distribution in the coastal

environments. Therefore, more studies are warranted to investigate the pollution of MPs with relatively smaller size in the coastal environments.

China possesses over 19,000 km of coastline, where more than 50% of the large cities and 40% of the population are concentrated (Luo, 2016). Qingdao, located on the Chinese northeast coast, is a highly urbanized coastal megacity, which covers an area of $11,293 \text{ km}^2$ along the coastline. Qingdao is a popular coastal tourist city, which is visited annually by millions of tourists. In addition, as an important “Blue Economic Zone” of China, Qingdao has nearly 10% of the national marine ranch demonstration area. Meanwhile, over 577 million tons of goods go through Qingdao’s ports every year, so that Qingdao is the international navigation hub in Northeast Asia and an international port city (Cao et al., 2020; Bie et al., 2021). Hence, the coastal environment in Qingdao is subjected to relatively high anthropogenic pressures (Figure 1), including large-scale aquaculture farming zones, international navigation port, famous tourist beaches, and scenic spots. However, several studies investigated the occurrence of MPs in the coastal environment of Qingdao. These results showed that the environmental factors (e.g., tidal residual currents, rainfall, winds, and eddies) were important factors affecting MP occurrence in Jiaozhou Bay, a semi-closed bay in Qingdao (Zheng et al., 2019; Liu et al., 2020). Meanwhile, Gao et al. (2021) emphasized the seasonal distribution in bathing

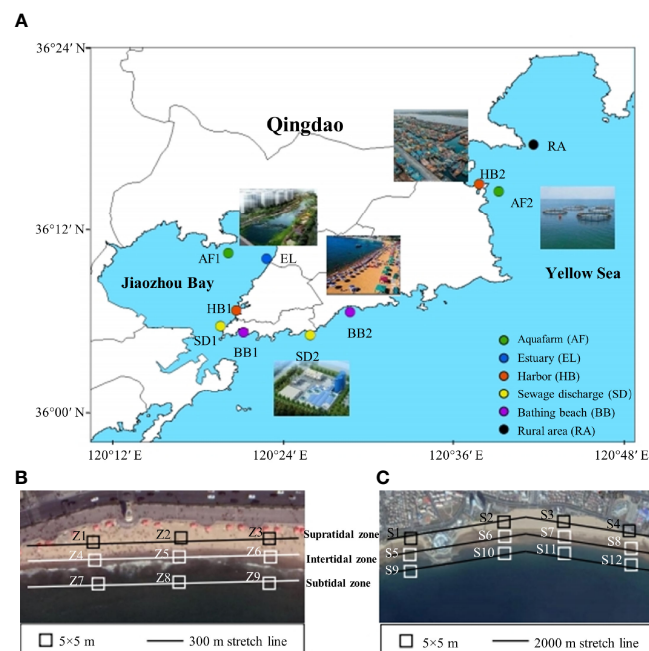


FIGURE 1 | The sampling zones along the coastal Qingdao (A) and their detailed information was provided in **Table S1**. Sampling sites within the scenic beach (BB1, B) and recreational beach (BB2, C). Site Z1–Z3 and S1–S4 were selected in the supratidal zone. Sites Z4–Z6, S5–S8 were selected in the intertidal zone, and sites Z7–Z9, S9–S12 were selected in the subtidal tidal. Sites S1, S5, and S9 were selected within the business and leisure areas. Sites S2, S6, and S10 were located close to the sewage outlet. Sites S3, S7, and S11 were located in the areas of bathing, and sites S4, S8, and S12 were located in undeveloped area. The five-point method was used for sampling sand samples from the beaches, and each sampling area was $5 \times 5 \text{ m}$. The solid line in the panel (B) represents 300 m stretch line in the scenic beach, and the solid line in the panel (C) represents 2000 m stretch line the scenic beach.

beaches of Qingdao. However, these studies paid little attention to the spatial distribution of MPs with smaller size ($< 330 \mu\text{m}$) in the seawater, sediment, and beach sand with the various anthropogenic activities in Qingdao's coastal environment.

Therefore, the seawater, sediment, and sand samples in 10 coastal zones with different anthropogenic activities in Qingdao coastal environment were selected. MPs were extracted from these environmental medias and the distribution characteristics (abundance, size, shape, color, and type) were observed and analyzed. The specific objectives of this study were to: (1) investigate the spatial distribution of MPs in seawater, sediment, and sand in Qingdao coastal environment; (2) assess the physicochemical characteristic diversities of MPs in different zones; (3) explore the relationship between MPs and various anthropogenic activities in coastal zones, and (4) distinguish the dominant factors affecting the MPs in the coastal environment. This study not only shone light on the effects of human activities on MP pollution in coastal cities, but also gave new insights in the fate of MPs in the coastal environment.

MATERIALS AND METHODS

Study Area

Ten sites in the coastal environment of Qingdao were selected based on different human activities (**Figure 1A**), including two aquafarms (AF1 and AF2), two sewage discharge outlets of WWTPs (SD1 and SD2), two harbors (HB1 and HB2), two bathing beaches (BB1 and BB2), and one estuary (EL) with municipal sewage (**Supplementary Table S1**). Sampling sites were close to the pollution sources or outfalls, such as ruins of abandoned aquafarm, surroundings of operational aquafarm, outfalls of WWTPs, docking areas of vessels, swimming areas of recreational beaches, hotspots of scenic beaches, and estuaries of rivers. AF1 was situated in an abandoned aquafarm with 30 years history, and AF2 was situated in a newly built aquafarm for 5 years. HB1 was located at the junction of a recreational, military and commercial harbor, while HB2 was located in a commercial harbor. SD1 was located close to the sewage discharge areas of Tuandao WWTP adopted traditional treatment process of anaerobic–anoxic–oxic treatment (A^2O). SD2 was located close to the Maidao WWTP adopted the membrane bio–reactor (MBR) process. BB1 and BB2 were situated in a scenic beach and recreational beach, respectively. EL was situated at the estuary of the Licun River, which is the longest river flowing through the densely populated areas of Qingdao. Moreover, the site RA located in a rural area with few anthropogenic impacts was selected as comparison. The detailed information including main hydrological and geographic characteristics of these sites is shown in **Supplementary Table S1**.

Sample Collection

All samples of seawater, sediment, and sand were collected in August 2018, which was the peak tourist season in Qingdao. A 50- μm mesh plankton net with 60-cm diameter circular opening was used to collect MPs in the subsurface seawater (Lenaker

et al., 2019). The amount of net submerged was kept a consistent submersion depth by monitoring the water inflow using a flowmeter (438–110, HYDRO–BIOS, Germany) mounted in the middle of the opening during the sampling duration of 15–30 mins. The time duration was chosen according to the same desired amount of water flowing through the network (Brignac et al., 2019). A global positioning system (GPS) was used to track boat position and course. Following the trawling, the net was hung on a homemade stainless–steel shelf and the net outside was sprayed using ultrapure water to remove the attached particulate matters (**Supplementary Figure S1**). Then, the particulate matters including MPs, organic debris, algae, and other pieces attached on the net walls were flushed into the net bottom. Following the flush, these particulate matters were transferred into a 1-L brown glass bottle by opening the valve at the net bottom and rinsing the particles with ultrapure water (Lenaker et al., 2019).

Surface sediments ($\sim 5 \text{ cm}$) were collected from each sampling site using a Peterson grab sampler (BJ Haifuda Technology Co., Ltd, China) (Leslie et al., 2017). Three buckets of sediments were collected at each sampling site and were composited in a stainless–steel salver for further homogenizing. Then the sediment was placed into an aluminum foil bag. All the foil bags were stored in storage boxes and transported to the laboratory in 12 h, and then stored at 4°C for further analysis.

Beach sand samples in the sites of BB1 and BB2 were collected following a method reported by Eo et al. (2018) with minor modifications. Three transects at each beach were sampled at locations at $\approx 1/4$, half–way, and $3/4$ along the length of BB1 (**Figure 1B**), which were perpendicular to the coastline (Brignac et al., 2019). In addition, four sampling groups were set perpendicular to the coastline in BB2 based on different human activities: (1) business and leisure areas (S1, S5, and S9); (2) sewage outlets (S2, S6, and S10); (3) bathing areas (S3, S7, and S11), and (4) the referenced area with little anthropogenic activity (**Figure 1C**). At each site, five sand samples were adopted using a ceramic shovel within a contour of $20 \times 20 \times 5 \text{ cm}$ (length \times width \times height). Subsequently, the sand samples in the same site were poured into pre–cleaned glass containers and adequately mixed with a stainless–steel scraper to make one homogenous composite sample. These sand samples were placed into aluminum foil bags for further transportation and stored at 4°C prior to analysis.

Extraction of MPs

Extraction of MPs from the sediment and sand samples coupled with density flotation with Fenton oxidation (Zhang et al., 2020; Liu Y., et al., 2021) was the method used, which is supported by the National Oceanic and Atmospheric Administration (NOAA) (Masura et al., 2015). Briefly, 100 g of the air–dried sediment or sand sample was placed in a beaker containing 600 mL of zinc chloride (ZnCl_2) solution (1.7 g/mL). Following stirring for 20 min with a glass bar and standing for 24 h, the upper aqueous phase containing MPs was collected. This extraction procedure was repeated three times and the upper aqueous were combined into a 1-L beaker. Then, the collected aqueous was filtered using a 5- μm nitrocellulose membrane to collect the particulate

matters, and then these particulate matters were scraped into a 100 mL beaker using a glass lens and digested using 60 mL Fenton's reagent (30% H₂O₂ with 5 mg ferrous iron catalyst) at 65°C for 72 h to remove organic material. Subsequently, the digested solution was filtered using a 0.45-μm nitrocellulose membrane, then the membrane was placed into a 60-mm petri dish, and air-dried at room temperature. Three treatments only containing ZnCl₂ solution without sediment or sand sample were set as control.

MPs were extracted from the seawater samples using a Fenton oxidation method (Prata et al., 2019). Briefly, the seawater sample was filtered using a 5-μm nitrocellulose membrane filter to collect particulate matters. Then, these particulate matters were scraped into a 100-mL beaker using a glass lens and digested using 60 mL Fenton's reagent at 65°C for 72 h. After that, the digestion was filtered using a 0.45-μm nitrocellulose membrane and then the membrane was placed into a 60-mm petri dish and air-dried. All membranes were stored in a dryer for further analysis.

Identification and Characterization of MPs

The particular matters collected on the membranes were microscopically analyzed to enumerate and categorize the inherent MPs according to morphology as fragments, fibers, pellets, and films (Lenaker et al., 2019). These particles were scanned using a fluorescent microscope equipped with a camera (DM2500, Leica, Germany) (Figure 2A). To confirm the polymer type of collected particles, a subset of MP samples collected from the seawater (20%, 509 particles), sediment (20%, 418 particles), and sand (10%, 335 particles) were selected for further analysis by micro-Fourier transform infrared (μ-FT-IR) spectroscopy (PerkinElmer Spectrum Spotlight 400, PerkinElmer Inc., US) (Ding et al., 2019). Polymer composition was determined by comparing the sample spectra to the standard spectra in the software using a matching-factor threshold of 0.80 (Figure 2B). Surface morphological characteristics of

MPs were determined using a scanning electron microscope (SEM, S-3400N, Hitachi, Japan) (Abbasi et al., 2021). MPs were attached to double-sided carbon tape, coated with a film of platinum, and then imaged at 15.0 kV in SE mode (Figures 2C–F).

Calculation of MP Diversity

Physicochemical characteristic diversity of MP communities in different zones could represent the difference in the source diversity (Li et al., 2020; Chen L. et al., 2021). Simpson diversity index (SDI), a comprehensive evaluation of richness and evenness, was used to assess the diversity of MPs in different zones. In the coastal environment MP system, the SDI was calculated for MPs of different sizes (SDI_{MPS}), shapes (SDI_{MPSH}), colors (SDI_{MPC}), and types (SDI_{MPT}). In addition, the MP diversity integrated index (MPDII), based on different diversity indices (Simpson-size, Simpson-shape, Simpson-color, and Simpson-polymer) of the MPs, was calculated to reflect the MP community composition and to indicate the number of pollution sources (Li et al., 2020). The specific calculation formula is as follows:

$$SDI = 1 - \sum_{i=1}^N P_i^2 \quad (1)$$

$$MPDII = (SDI_{MPS} \times SDI_{MPSH} \times SDI_{MPC} \times SDI_{MPT})^{1/4} \quad (2)$$

where P_i is the proportion of category i MPs in total samples ($P_i = \frac{N_i}{N}$) N is the number of categories (e.g., $N = 8$, indicating 8 types of MPs were detected in this study; $N = 7$, indicating 7 colors of MPs were detected in this study; $N = 4$, indicating 4 shapes of MPs were detected in this study); and i is the index of categories from 1 to N . Thus, richness is expressed as the term N , while balance is captured by the variation in values of P across i categories.

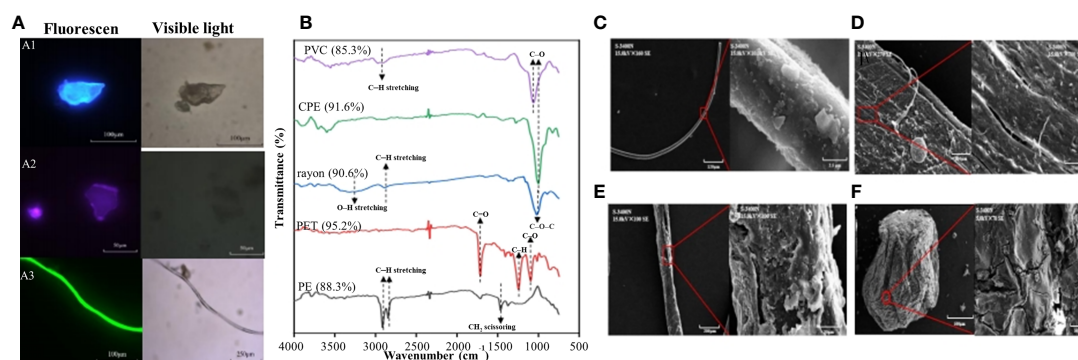


FIGURE 2 | The representative microscopic images of MPs collected from the seawater, sediment and sand samples (A). The fragment was collected from seawater in AF1 (A1), the pellet and film were collected from sediment in EL (A2), and the fiber was collected from seawater in SD2 (A3). The representative μ-FTIR spectra of MPs collected from the coastal zone (B). Among them, the PVC was collected from sediment in EL, the CPE and rayon were collected from seawater in SD2, the PET and PE were collected from seawater in AF1. The proportion above each spectral line is the similarity between the target polymer and the standard polymer in the library. SEM images of the representative MPs collected from seawater in sewage discharge area (SD2) (C) and harbor (HB1) (D), sediment in sewage discharge area (SD2) (E), and sands in bathing beach (BB2) (F).

Quality Assurances (QA) and Quality Controls (QC)

All samples were collected by metal or ceramic samplers and stored in glass containers to avoid possible contamination. All glass containers were soaked with dilute sulfuric acid (10%) overnight and then rinsed 5 times with ultrapure water before use. The relevant sampling tools were thoroughly rinsed with ultrapure water at each site before sampling. Triplicate samples from each site were taken randomly and the mass of each sample was guaranteed equally. All chemical reagents were filtered through 0.22- μm nitrocellulose filter membranes. The flotation separation and extraction of MPs should be ensured that all the open instruments are sealed with tin foil. Simultaneously, ultrapure water was added to a flask without sediment sample as a procedural blank. The results showed that the average abundance of MPs in the blank samples was 1.7 items, much lower than those detected in environmental samples, indicating that the results were reliable. The recovery rates of the pretreatment processes were determined with standard MP samples, which ranged from 88.3–92.5% (details are presented in the **Supplementary Material**).

Statistical Analysis

Each sediment sample was performed in triplicate, and the MP abundance was expressed as mean values \pm standard deviation ($n = 3$). All abundance data were tested by one-way analysis of variance (ANOVA), which was adopted to compare the mean values and relative standard deviation of the replicates. Differences were considered significant at $P < 0.05$. The correlations between the MP abundance, the distribution of MPs, and different human activities were analyzed using statistical product and service

solutions software (SPSS 20.0). Map figures were constructed using ArcGIS (Version 10.2, ESRI).

RESULTS

Occurrence of MPs in the Coastal Surface Seawater

MPs were detected in all the surface seawater samples collected from all 10 zones stressed by different human activities (**Figure 3A**). The abundance levels ranged from 23.8 to 259 items/ m^3 , with an average abundance of 93.1 ± 63.5 items/ m^3 ($n = 30$). Their average abundances followed an order of AF1 (230 ± 39.9 items/ m^3) > HB1 (162 ± 18.7 items/ m^3) > HB2 (108 ± 7.7 items/ m^3) > BB2 (93.1 ± 17.5 items/ m^3) > BB1 (75.3 ± 14.6 items/ m^3) > EL (75.1 ± 3.0 items/ m^3) > SD2 (56.9 ± 11.9 items/ m^3) > SD1 (44.4 ± 4.8 items/ m^3) > AF2 (30.5 ± 3.0 items/ m^3) \approx RA (28.0 ± 3.6 items/ m^3). Obviously, the highest abundance of MPs in seawater along the Qingdao coastal environment was detected in the abandoned aquafarm (AF1), followed by harbors, beaches, estuary, sewage discharge areas, operational aquafarm (AF2), and rural area (**Figure 3B**). The abundance of MPs in abandoned aquafarm (AF1) was an order of magnitude higher than that in the operational aquafarm (AF2). In addition, little significant difference in the MP abundances was observed for other zones with the same human activities, such as harbors, beaches, and sewage discharge areas.

The small fragments with size of 50–100 μm were the dominant MP type in the seawater (**Supplementary Figure S2A**), accounting for 62.6–82.4%, followed by those of 100–300 μm (9.57–33.3%), 300–1000 μm (1.70–6.19%), and 1000–5000 μm (1.16–4.62%) (**Supplementary Figure S2B**). The color of detected MPs was mainly transparent (38.5%) and white (26.5%)

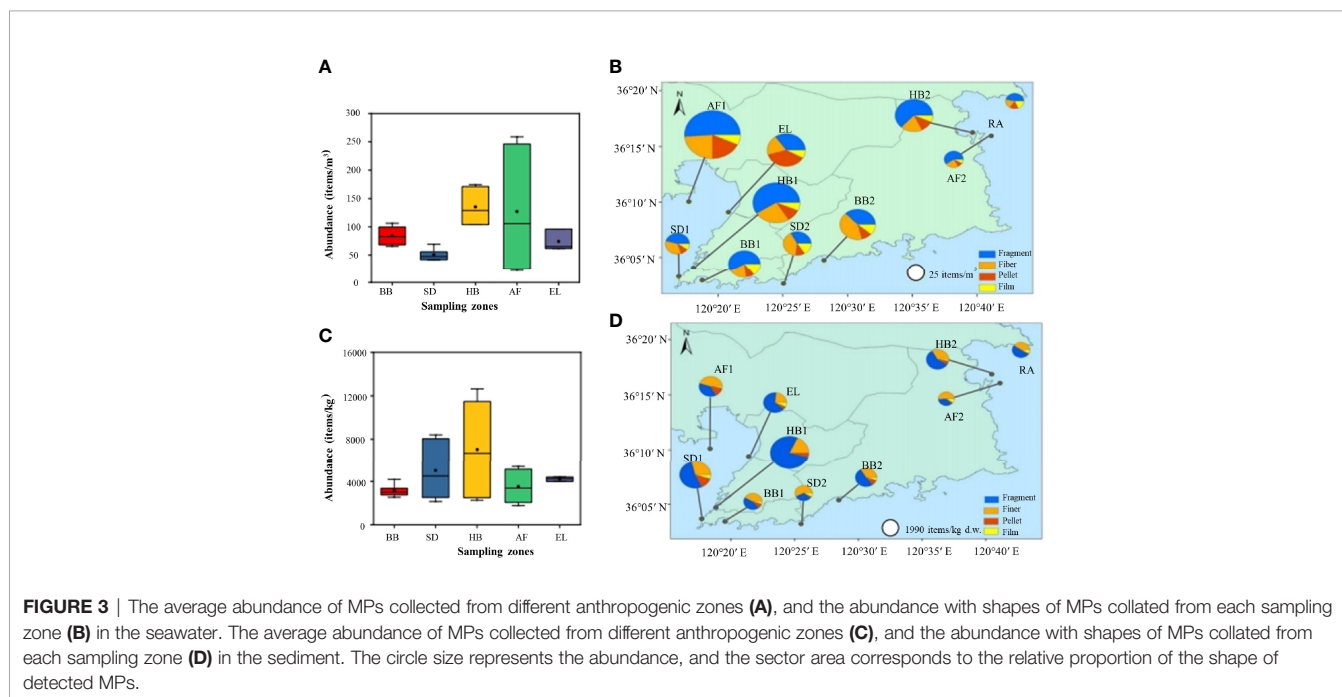


(**Figure 4A**). In addition, the proportion of green MPs was higher in the two beaches (9.33–12.4%) and the two sewage treatment plants (9.82–10.0%) than other coastal zones, while the proportion of yellow MPs was higher in the abandoned aquafarm (AF1, 11.5%), estuary (EL, 12.5%), and harbor (HB2, 14.1%). Moreover, many red MPs were found in the rural area (RA, 26.2%) (**Figure 4B**). The distribution of different shapes of MPs varied among the coastal zones with different human activities (**Figure 3A**). For example, fiber accounted for 33.8–40.6% of the total detected MPs in the sewage discharge areas (SD1, SD2) and 41.2% in the recreational bathing area (BB2), while pellets accounted for 36.4% in the estuary of the Licun River (EL). Moreover, fragments were dominant in harbors (60.0–71.9%) and scenic beaches (BB1, 58.5%).

Eight polymer types of MPs were identified in all the seawater samples (**Figure 5A**), including polyethylene (PE), chlorinated polyethylene (CPE), rayon, polystyrene (PS), polyethylene terephthalate (PET), polyvinyl chloride (PVC), polypropylene (PP), and poly tetra fluoroethylene (PTFE). In the estuary zones (EL), PS accounted for the largest proportion of 30.3%, followed by CPE (24.2%), PE (13.6%), rayon (10.6%), PVC (10.6%), PET (6.06%), PP (3.03%), and PTFE (1.52%). In the two sewage treatment plants (SD1, SD2), the proportion of rayon was higher (19.5–31.3%), while in the abandoned aquafarms (AF1), the proportion of PVC was higher (21.4%). Compared with other zones, the types of MPs detected in the two beaches and harbors were more abundant, especially the PTFE detected in BB1 and SD2. In rural areas, CPE was the main type (28.0%), followed by

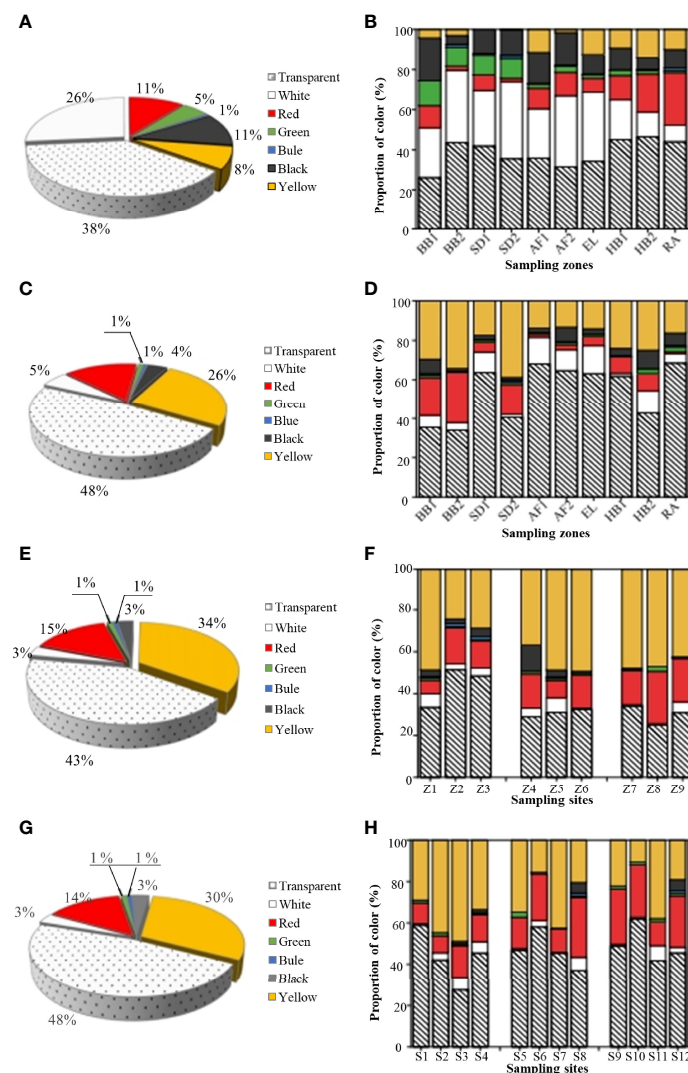


FIGURE 4 | The average abundance of MPs with different colors collected from all zones (**A**), and the color distribution from each sampling zone (**B**) in the seawater. The average abundance of MPs with different colors collected from all zones (**C**), and the color distribution from each sampling zone (**D**) in the sediment. The average abundance of MPs with different colors collected from sand samples collected from BB1 (**E**) and BB2 (**G**), and the color distribution from each sampling site (BB1, **F**; BB2, **H**). Site Z1–Z3 and S1–S4 in the supratidal zone. Site Z4–Z6 and S5–S8 in the intertidal zone. Site Z7–Z9 and S9–S12 in the subtidal zone.

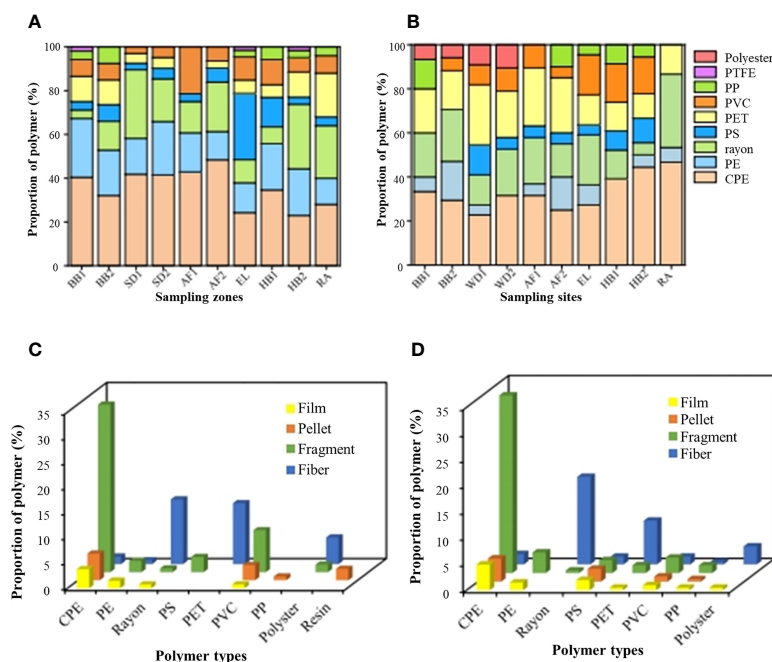


FIGURE 5 | The polymer composition of MPs in the seawater (A) and sediment samples (B) collected from each sampling zone. Relative proportion of MPs classified by the morphological types in the BB1 (C) and BB2 (D). PE, polyethylene; CPE, chlorinated polyethylene; PP, polypropylene; PS, polystyrene; PET, polyethylene terephthalate; PVC, polyvinyl chloride and PTFE, poly tetra fluoroethylene.

rayon (24.0%), PE (12.0%), PET (20.0%), PVC (8.00%), PP (4.00%), and PS (4.00%).

Depositional Distribution of MPs in the Coastal Sediments

MPs were detected in all the sediment samples collected from the 10 zones in the Qingdao coastal environment subjected to different human activities (Figure 3C). The abundance levels of MPs ranged from 1540–12603 items/kg, and the average abundance was 4577 ± 2902 items/kg ($n = 30$). Their average abundances followed an order of HB1 (11603 ± 971 items/kg) > SD1 (7627 ± 1043 items/kg) > EL (4249 ± 186 items/kg) > AF1 (4113 ± 101 items/kg) > HB2 (4020 ± 2155 items/kg) > BB2 (3567 ± 550 items/kg) > BB1 (2712 ± 161 items/kg) > RA (2487 ± 220 items/kg) > SD2 (2410 ± 235 items/kg) > AF2 (1989 ± 101 items/kg). The highest MP abundance of sediments was in the harbor, followed by sewage discharge, estuary, abandoned aquafarm, beaches, rural area, and operational aquafarm (Figure 3D).

In all coastal zones, MPs with the smallest size category (50–100 μm) were dominant, accounting for 46.7–85.4% of the total recovered MPs, followed by the size of 100–300 μm (8.83–35.0%), 300–1000 μm (2.77–19.4%), and 1000–5000 μm (2.49–9.93%) (Figures S2C, D). Transparency (48.2%) was also the main color of the detected MPs in the sediments (Figure 4C). But the other color distribution of MPs varied among the coastal zones with different human activities (Figure 4D). For example, the yellow MPs were more frequently recovered in the two beaches (29.6–

34.2%), two harbors (23.9–24.1%), and sewage discharge area (SD2, 38.8%). Comparatively, the proportion of white MPs was higher in the two aquafarms (10.4–13.5%), sewage discharge area (SD1, 10.4%), and harbor (HB, 14.2%). In addition, the red MPs accounted for 19.6–26.0% in the two beaches and 15.6% in the sewage discharge area (SD2). Similar to the seawater samples, the proportions of different MP shapes showed significant changes across the different zones (Figure 3D). For example, the proportion of fiber followed an order of sewage discharge area (SD2, 57.5%), the two aquafarms (44.9–51.2%), recreational beach (BB2, 41.7%), and rural area (RA, 40.2%). Fragments were predominant in the estuary (EL, 65.1%), two harbors (58.2–77.4%), and scenic beach (BB1, 52.3%). The proportion of pellets in sewage discharge area (SD1, 13.3%) and abandoned aquafarm (AF1, 14.8%) were higher, while the proportion of films was higher in the aquafarm (AF2, 9.4%). In addition, compared with the seawater samples, the proportion of fiber in sediment increased significantly.

Eight component types of MPs were identified in all the sediment samples, including PE, CPE, rayon, PS, PET, PVC, PP, and polyester. Compared with the seawater samples, PTFE was not observed in all the sediments, but polyester fibers were detected (Figure 5B). Among them, the proportion of PET in the two sewage discharge areas (21.0–27.3%) and two aquafarms (25.0–26.3%) were relatively higher than other zones. Moreover, the polyester fibers were only detected in the sewage discharge areas (9.09–10.5%) and beaches (5.9–6.7%). In addition, the proportion of PVC in the estuary (EL, 18.2%) and two harbors

(16.7–17.4%) was larger than the other zones. Except for the sewage discharge area (SD1, 13.6%) and harbor (HB2, 11.1%), PS accounted for less than 10% in other zones. Furthermore, CPE (46.7%), PE (6.67%), rayon (33.3%), and PET (13.3%) were only detected in the rural area.

Spatial Variations of MP Abundances in the Coastal Beaches

The abundances of MPs in the two beach sands ranged from 1137–8537 items/kg (Figure 6), with the average abundance of 3602 ± 1708 items/kg ($n = 63$). Both the highest and the lowest abundance were detected at S1 (the supratidal zone of the business and leisure area) and S8 (the intertidal zone of the remote area) in the BB2 (Figures 6A, B). Interestingly, the distribution characteristics of MPs in the supratidal zone, intertidal zone, and subtidal zone of these two bathing beaches were significantly different. As a recreational beach for tourism, MP pollution in BB1 was concentrated at S1–S4 in the supratidal zone with the abundance of 5805 ± 1091 items/kg (Figure 6C), whereas the highest abundance of MPs in BB2 was found at Z4–Z6 in the intertidal zone with the abundance of 5227 ± 1482 items/kg (Figure 6D).

In all the tidal zones of two beaches, the abundances of MPs with the smallest size category (50–100 μm) were the highest (61.5–69.7%), followed by the size of 100–300 μm (14.4–15.7%), 1000–5000 μm (8.93–11.3%), and 300–1000 μm (6.93–11.4%) (Supplementary Figures S2E, F). Among them, the intertidal

zone of the bathing area in BB2 was dominated by the larger MPs with sizes of 1000–5000 μm (S7, $50.6 \pm 9.83\%$), but other sites were still dominated by the smaller MPs with sizes of 50–100 μm (42.2–85.6%) (Supplementary Figures S2G, H). The color patterns of MPs in the two beaches were consistent. The largest proportion of MPs in the two beaches was transparent, accounted for 42.9–47.5%, followed by yellow (30.5–34.6%), red (13.9–14.7%), white (3.10–3.11%), black (2.99–3.12%), green (0.99–1.07%), and blue (0.77–0.82%) (Figures 4E, F). Moreover, the proportion of yellow MPs in the zones for bathing and sewage outlet (S2, S3, S7, and S11) were higher than other sites in BB2. However, for BB1, the transparent MPs were dominant in the supratidal zone (33.6–52.5%), and the yellow MPs were dominant in the intertidal zone (39.1–49.1%) and subtidal zone (43.3–48.4%) (Figure 4G). By contrast, for BB2, the yellow MPs had a higher proportion in the supratidal zone (27.1–50.2%), and transparent MPs were dominant in the intertidal zone (38.2–55.5%) and subtidal zone (42.4–58.0%) (Figure 4H).

In these two coastal beaches, the shapes of recovered MPs included fragment, fiber, pellet, and film. The fragments showed the highest abundance with a proportion of 49.8% in BB1, especially in the intertidal zone (40.5–72.8%), followed by the subtidal zone (43.2–45.4%), and supratidal zone (28.8–32.4%) (Figure 6C). However, fibers were the dominant MPs (20.5–92.3%) in BB2, especially in the intertidal zone (40.7–92.3%), followed by the subtidal zone (43.8–65.0%), and supratidal zone (20.5–42.3%) (Figure 6D). Moreover, the proportion of

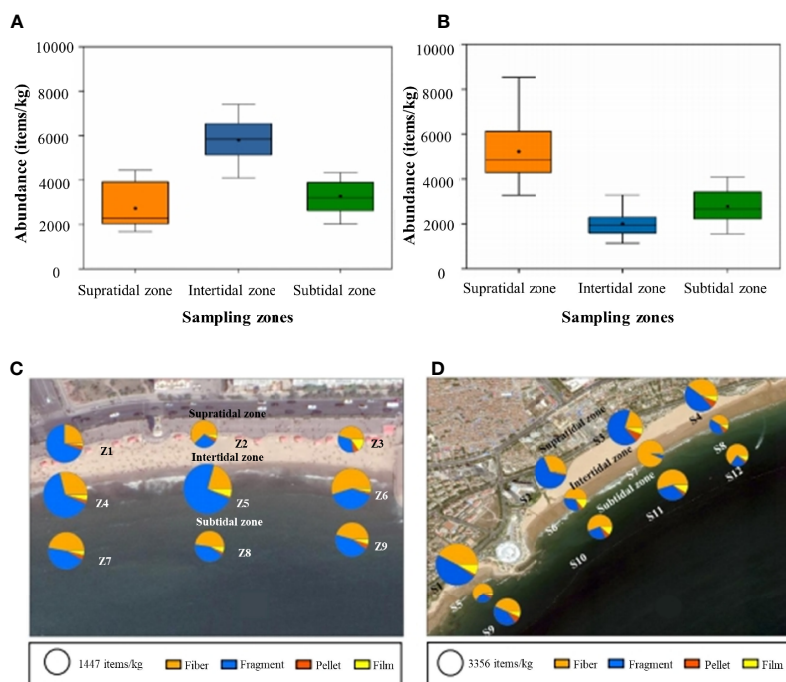


FIGURE 6 | The abundance and shape of MPs in the sand samples collected from BB1 (A, C) and BB2 (B, D). Sites Z1–Z3 and S1–S4 were located in the supratidal zones. Sites Z4–Z6 and S5–S8 were located in the intertidal zones, and sites Z7–Z9 and S9–S12 were located in the subtidal zones. Sites S1, S5, and S9 were selected within the business and leisure areas. Sites S2, S6, and S10 were located close to the sewage outlet. Sites S3, S7, and S11 were located in the areas of bathing, and sites S4, S8, and S12 were located in the zone with less human activities. The size of the circle represents the concentration, and the area of the sector corresponded to the proportion of the shape.

fragments was higher in the supratidal zone (47.0–66.0%) relative to other sites in BB2. In addition, the distribution patterns of MP shapes were also related to the different human activities. For example, in the scenic beach (BB1), the proportion of fiber was 64.8–72.8% at the sites of Z2, Z3, and Z6 located in the scenic spot, higher than those at other sites in the rural area and business area. However, the fragments were more prevalent at Z1 and Z4, the remote area in the BB1. In the recreational beach (BB2), the proportion of fiber was 92.3% and 63.2% at S7 and S5, located in the business, leisure, and swimming zone of the beach, respectively. Furthermore, the proportion of fragments was 66.2% and 65.3% at S3 and S2, respectively, located in the camping and sewage outlet zones of the beach. The proportion of films and pellets was 14.1% and 8.87% at S6 and S2, respectively, the sewage outlet and camping zones.

Seven component types of MPs were identified in all the sand samples, including PE, CPE, rayon, PS, PET, PVC, and PP (Figures 5C, D), consistent with those in the coastal sediments. Among them, CPE was dominant in BB1 (46.4%) and BB2 (45.3%), followed by rayon (15.2%), PET (14.4%), PVC (12.8%), PE (7.20%), PS (3.20%), and PP (0.80%) in BB1, and rayon (17.2%), PET (14.3%), PS (8.37%), PVC (6.40%), PE (5.42%), and PP (2.96%) in BB2. In addition, the foam particles with sizes of 1000–5000 μm

in the BB2 were identified as expandable polystyrene (EPS) (Figure 2C).

Diversity of MP Communities

In the present study, SDI was used to estimate the diversity of MP communities in terms of size, color, shape, and type. The SDI of size (SDI_{MPS}), color (SDI_{MPC}), shape (SDI_{MPSH}), and type (SDI_{MPT}) were 0.34–0.43, 0.66–0.78, 0.52–0.68, and 0.59–0.77, respectively. The values significantly varied among the seawater samples in different zones (Figure 7A). Among them, the highest SDI_{MPS} was in EL (0.43 ± 0.07), followed by SD (0.40 ± 0.08), RA (0.39 ± 0.09), AF1 (0.38 ± 0.05), BB (0.38 ± 0.04), AF2, (0.34 ± 0.06), and HB (0.31 ± 0.16) (Figure 7A). The value of SDI_{MPC} followed an order of AF2 (0.73 ± 0.00) > BB (0.72 ± 0.08) > AF1 (0.71 ± 0.04) \approx EL (0.71 ± 0.06) > RA (0.70 ± 0.02) \approx SD (0.70 ± 0.05) > HB (0.68 ± 0.06). In terms of SDI_{MPSH} , the highest value was 0.68 ± 0.02 in AF2, followed by EL (0.66 ± 0.05), SD (0.66 ± 0.03), BB (0.63 ± 0.07), AF1 (0.59 ± 0.16), RA (0.56 ± 0.11), and HB (0.52 ± 0.12). In addition, the value of SDI_{MPT} followed an order of HB (0.77 ± 0.03) \approx EL (0.77 ± 0.01) > BB (0.73 ± 0.03) > SD (0.69 ± 0.04) > AF1 (0.64 ± 0.03) > RA (0.63 ± 0.05) > AF2 (0.59 ± 0.03). These results indicated that the sources of MPs were more complex in the operational aquafarm, beaches, and estuary than the other coastal zones in Qingdao.

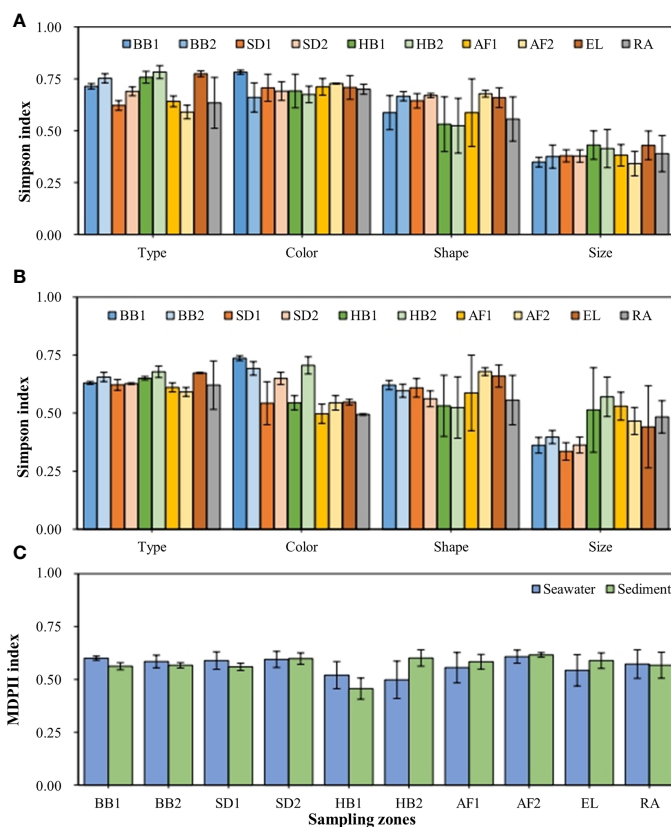


FIGURE 7 | Simpson index of MP communities in seawater (A), sediments (B) at different sampling zones from the coastal Qingdao, including the diversity index of types, colors, shapes, and size. MP diversity integrated index (MPDI) in different sampling zones (C). Error bars represent standard deviations of the means ($n = 3$).

The results of MPs diversity in the sediments were similar to those in seawater (**Figure 7B**). The value of SDI_{MPS} followed an order of $AF1 (0.53 \pm 0.06) \approx SD (0.53 \pm 0.08) > RA (0.48 \pm 0.07) > AF2 (0.47 \pm 0.06) > EL (0.44 \pm 0.06) > HB (0.40 \pm 0.18) > BB (0.37 \pm 0.04)$. In terms of SDI_{MPC} , the highest value was 0.71 ± 0.03 in BB, followed by HB (0.62 ± 0.09), SD (0.59 ± 0.08), EL (0.55 ± 0.01), AF2 (0.54 ± 0.02), AF1 (0.50 ± 0.04), and RA (0.49 ± 0.00). For SDI_{MPSH} , the highest value was 0.68 ± 0.02 in AF2, followed by EL (0.66 ± 0.04), BB (0.61 ± 0.02), AF1 (0.59 ± 0.16), SD (0.58 ± 0.04), RA (0.56 ± 0.11), and HB (0.53 ± 0.12). For SDI_{MPT} , the highest value was 0.67 ± 0.00 in EL, followed by HB (0.66 ± 0.02), BB (0.64 ± 0.02), RA (0.62 ± 0.10), SD (0.62 ± 0.02), AF1 (0.61 ± 0.02), and AF2 (0.59 ± 0.02). These results indicated that the higher diversity of MPs was in the abandoned aquafarm, harbors, and estuary than the other coastal zones in Qingdao.

The highest SDI_{MPS} values for the sand samples in BB1 were observed in the subtidal zone (0.53–0.56), followed by the intertidal zone (0.41–0.52) and the supratidal zone (0.30–0.40) (**Supplementary Figure S3A**). Moreover, the highest values of SDI_{MPS} in BB2 were found in the intertidal zone (0.51–0.65), followed by the subtidal zone (0.36–0.59) and the supratidal zone (0.25–0.59) (**Supplementary Figure S3B**). For SDI_{MPC} , the highest values in BB2 were observed in the subtidal zone (0.61–0.67), followed by the intertidal zone (0.59–0.65) and the supratidal zone (0.60–0.63), while the values in BB1 in the subtidal zone (0.61–0.66) were slightly higher than the intertidal zone (0.61–0.66) and the supratidal zone (0.61–0.65). The two beaches showed the same trend of SDI_{MPSH} (**Supplementary Figures S3A, B**). The highest value was observed in the subtidal zone (BB1, 0.56–0.58; BB2, 0.50–0.62), followed by the supratidal zone (BB1, 0.43–0.62; BB2, 0.49–0.60) and the intertidal zone (BB1, 0.37–0.53; BB2, 0.14–0.64). Moreover, the highest values of SDI_{MPT} were found in BB1 in the intertidal zone (0.65–0.74), followed by the supratidal zone (0.62–0.74) and the intertidal zone (0.63–0.70), and which was found in BB2 was 0.54–0.81 in the subtidal zone, followed by the intertidal zone (0.43–0.74) and the supratidal zone (0.44–0.70). However, the MPDI values, ranging from 0.46–0.62 did not differ in seawater, sediment (**Figure 7C**), or sand (BB1) samples, indicating the presence of different complexity in the MP characteristic compositions and abundance variations of these regions (**Supplementary Figure S3C**). Moreover, the MPDI values were much lower at the sites (S3, S7) in the bathing area (0.39–0.43) than the other sites in BB2 (**Supplementary Figure S3D**), indicating that the MP source was relatively simpler in the bathing areas than those in the business area and sewage outlet area in the beach.

DISCUSSIONS

Comparison of MP Pollution in the Qingdao Coastal Environment With Coastal Zones Around the World

A simple comparison of MP concentrations with several previously reported values for seawater in the coast is summarized in **Table 1**. The average MP abundances in seawater of coastal Qingdao (93.1 ± 63.5 items/m³) were lower

than most of those reported in the global coastal regions, including the developed coastal regions such as South Korea (290 ± 210 – 1570 ± 1330 items/m³) and Germany (4137 ± 2461 items/m³), and the less developed coastal regions such as South Africa (258 ± 53.4 – 1215 ± 278 items/m³) and Indonesia (485 items/m³) (Nel and Froneman, 2015; Cordova et al., 2019; Mani et al., 2019; Jung et al., 2020). Similarly, the level of MP pollution in the coastal seawater of Qingdao was lower than most of those investigated in the domestic coastal regions, such as Xiamen (514 ± 520 items/m³) and Maowei Sea (4500 ± 100 items/m³). However, the average MP abundance of seawater in Qingdao was higher than that in west coastal India (0.11 ± 0.03 items/m³) (Gupta et al., 2021) (**Supplementary Figure S4A**). As an important coastal tourism city in China, Qingdao has developed recreational tourism, international harbors, and numerous aquaculture industries (Liu et al., 2020; Bie et al., 2021), resulting in the pollution of MPs in the coastal environment from the aging aquaculture facilities, packing waste, and abrasion of tires (Xue et al., 2020). Thus, the increasing urbanization generally exacerbates plastic pollution due to the growing waste and wastewater drainages from recreational activities and industrial development. Moreover, the mismanaged plastic waste probably increased MP pollution in coastal cities (Rochman and Hoellein, 2020). For example, the MP abundance in Qingdao Harbor (108 – 162 items/m³) was lower than the Lamong Bay in Indonesia (380 – 610 items/m³) (Cordova et al., 2019). They explained that Lamong Bay was surrounded by harbor activities and settlements, and the high population activities on the upstream river and frequent navigation resulted in a large number of MPs arbitrarily discharged into the waters. The relatively lower MP abundance in the harbors of Qingdao was due to low community activities as far away from residential areas. In addition, the MP abundance in Qingdao beaches (75.3 – 93.1 items/m³) was lower than the Kenjeran Beach in Indonesia (460 – 550 items/m³), where the local residents arbitrarily discard household waste directly into the seawater and beach sand because of little temporary landfill (Cordova et al., 2019). Additionally, previous studies found that sampling with a mesh smaller than 100 μ m in size increased MP abundance by 1–4 orders of magnitude relative to those using the standard 330 μ m mesh (Prata et al., 2019; Jung et al., 2020; Watkins et al., 2021). Thus, in the present study, a 50- μ m mesh plankton net was used to collect MPs in seawater, the mesh size much smaller than most of the reported studies (330 μ m), thus the abundance of MPs in Qingdao coastal seawater should be higher than those of other regions. This disagreed with the results in the present study, implying the relatively low level of MP pollution in the Qingdao coastal surface water.

The abundances of MPs in the coastal sediments and sands were generally higher than those in the majority of global and domestic coastal regions (**Table 1**). For example, the MP abundance in coastal sediments of Qingdao (4577 ± 2902 items/kg) was higher than those in Brittany (France) (1.53 ± 2.84 items/kg), Rias Baixas (Spain) (70.2 ± 74.2 items/kg), Sanggou Bay (China) (1674 ± 526 items/kg), and the southwestern coast of Taiwan (China) (29.4 ± 40.7 items/kg) (Thomas et al., 2017; Carretero et al., 2020; Sui et al., 2020;

TABLE 1 | Summary of MP pollution in seawater, sediment, and sand in coastal regions around the world.

Study area ^a	Marine medium	Size	Abundance ^b	Main shape	Reference
Bohai	Seawater	0.3–0.5 mm	0.4 ± 0.1 items/m ³	Fiber	(Zhao et al., 2018)
South China Sea	Seawater	0.02–0.30 mm	0.05 ± 0.09–2569 ± 1770 items/m ³	Fiber	(Cai et al., 2018)
Xiamen	Seawater	< 5 mm	514 ± 520 items/m ³	Granule and foam	(Tang et al., 2018)
South Africa	Seawater	0.065–5 mm	258 ± 53.4–1215 ± 277 items/m ³	Fiber	(Nel and Froneman, 2015)
Korea	Seawater	0.02–5 mm	20–4280 items/m ³	Fragment and fiber	(Jung et al., 2020)
Maowei Sea	Seawater	0.25–5 mm	4500 ± 100 items/m ³	Fiber	(Zhu et al., 2019)
Israel Gulf Coast	Seawater	0.3–5 mm	7.68 ± 2.38–69.6 ± 128 items/m ³	Fragment	(Hal et al., 2017)
Germany	Seawater	0.5–5 mm	4137 ± 2461 items/m ³	Fiber	(Mani et al., 2019)
India	Seawater	0.02–5 mm	0.06–0.18 items/m ³	Fragment	(Gupta et al., 2021)
Indonesia	Seawater	0.3–1 mm	130–890 items/m ³	Foam	(Cordova et al., 2019)
Jiaozhou Bay	Seawater	0.1–4mm	46 ± 28 items/m ³	Fiber	(Zheng et al., 2019)
Qingdao	Seawater	0.05–5 mm	93.1 ± 63.5 items/m ³	Fragment	The present study
Bohai	Sediment	66.25 µm–4.98 mm	172 items/kg	Fiber	(Zhao et al., 2018)
North Yellow Sea			124 items/kg		
Southern Yellow Sea			72.0 items/kg		
Xiamen	Sediment	< 5 mm	181 items/kg	Fiber	(Tang et al., 2018)
Japan	Sediment	0.3–5 mm	1845–5385 items/kg	Fragment	(Matsuguma et al., 2017)
Iran	Sediment	< 5 mm	295–1085 items/kg	Fragment	
Durban	Sediment	0.2–5 mm	2400 ± 529–111933 ± 29189 items/kg		(Preston et al., 2021)
Sanggou Bay	Sediment	< 0.5 mm	1674 ± 526 items/kg	Granule and film	(Sui et al., 2020)
Germany	Sediment	11–500 µm	260 ± 10–11070 ± 600 items/kg		(Mani et al., 2019)
Coastal plain river network in eastern China	Sediment	0.1–5 mm	32947 ± 15342 items/kg	Fragment	(Wang et al., 2018)
Yangtze River	Sediment	0.333–5mm	34 items/kg		(Xiong et al., 2019)
Southwestern coast of Taiwan in China	Sediment	0.1–1 mm	29.4 ± 40.7 items/kg	Fiber	(Chen et al., 2021)
India	Sediment	0.5–1 mm	24.5 ± 5.64–235 ± 64.4 items/kg	Fiber	(Sathish et al., 2020)
Brittany	Sediment	0.21–1 mm	1.53 ± 2.84 items/kg	Pellet	(Frère et al., 2017)
Spain	Sediment	0.5–1 mm	70.2 ± 74.2 items/kg	Fiber	(Carretero et al., 2020)
Jiaozhou Bay	Sediment	0.1–4mm	15 ± 6 items/kg	Fiber	(Zheng et al., 2019)
Qingdao	Sediment	0.05–5mm	4577 ± 2902 items/kg	Fragment	The present study
Southeastern United States (eighteen NPS ^c)	Sand	>0.01mm	42–443 items/kg	Fiber	
Beibu Gulf	Sediment	< 5 mm	6923 ± 2566 items/kg		(Qiu et al., 2015)
Southeastern coast of India	Sand	>0.01mm	153 ± 27.3–378 ± 39.7 items/kg	Fragment	(Patchaiyappan et al., 2021)
Spain	Sand	< 5 mm	22.0 ± 23.2–45.0 ± 24.7 items/kg	Fragments and spheres	
Slovenian beaches	Sand		10.9 ± 23.2 items/kg	Fibres	
Mumbai	Sand	< 5 mm	45 ± 12–220 ± 50 items/kg	Fiber	(Tiwari et al., 2019)
Phuket	Sand	0.02–5mm	188 ± 34 items/kg	Fiber	(Akkajit et al., 2021)
Qingdao	Sand	0.05–5mm	3602 ± 1708 items/kg	Fragment	The present study

^aSelected study area include aquaculture areas, wastewater treatment plants, estuaries, and harbors in developed areas and developing areas.

^bSelected studies were those which quantified specifically MPs and provided sufficient methodological details to allow for conversion of units, to standardise by volume for comparability.

^cNPS : National Park Service.

Chen L., et al., 2021) (**Supplementary Figure S4B**). However, the abundance in Qingdao was lower than that in Durban (South Africa) (2400 ± 529–111,933 ± 29,189 items/kg) (Preston et al., 2021), mainly due to the good management for recycling and disposal of plastic waste. Particulate matters (e.g., MPs, algae, sands) were preferentially settled in low-dynamic aquatic environments because the strong hydrodynamic force impedes MP sedimentation and deposition in sediment environments (Xue et al., 2020; Gupta et al., 2021). The sediments are likely to be the important sinks of MPs due to their deposition and weak hydrodynamic conditions in the semi-enclosed bays, being unfavorable for the long-distance migration of MPs in the coastal environment (Sun et al., 2020). For example, the average MP abundance in the harbors of Qingdao was much

higher (7813 ± 4413 items/kg) than those in Göteborg Harbor (Sweden) (810 ± 210 items/kg) and Greater Melbourne (Australia) (4.50–173 items/kg) (Su et al., 2020). This was mainly ascribed to the weaker water exchanges of the harbors located in the semi-enclosed bay of Jiaozhou compared to those harbors located in Puerto Montt (Chile, 40 ± 69.28 items/kg) and Itaipu Embayment (Australia, 20.3 items/kg) with high hydrodynamics (Castro et al., 2020; Jorquera et al., 2022), implying that lentic waterbodies could be a sink for MPs due to low flow rates and wave energy. Furthermore, the MP occurrence in coastal environments was largely determined by anthropogenic forces. For example, the harbors in Qingdao are mainly used for transportation and international trade, resulting in the heavier MP pollution in Qingdao than that of Chalong Pier

in Phuket (36.4 ± 17.0 – 82.2 ± 32.4 items/kg), which is mainly serviced for tourists (Akkajit et al., 2021). For beach sands, the recreational activities clearly determined MP prevalence on the beaches in this study, which was supported by the lower MP abundance on the scenic beach (BB1) than the recreational beaches (BB2) (**Figure 1**). The sources of MPs within BB2 could be water recreations such as swimming, surfing, camping, water-skiing, fishing, and food outlets (Pervez et al., 2020). The average MP abundance in the beaches of Qingdao (3937 ± 1667 items/kg) was much higher than those in Phuket, Thailand (188 ± 34 items/kg) and Serenity Beach, India (1357 ± 120 items/kg), where the beaches are mainly serviced for fishing activity (Dowarah and Devipriya, 2019; Akkajit et al., 2021) (**Supplementary Figure S4C**). Certainly, it is worth noting that the deposition of MPs in the coastal environment can pose great ecological risks on the aquatic ecosystems, thus the potential environmental risks of MP pollution in these different coastal environments should be carefully examined.

Influence of Human Activities on the Distribution Patterns of MPs in Coastal Qingdao

The differences of human activities in coastal cities, including tourism, aquaculture, navigation, fishery, and urban sewage discharge, are highly related with the degree of urbanization and industrialization. Frequent human activities will lead to differences in the abundance and types of exogenous pollutants (e.g., trace metals, PPCPs, and MPs) in the coastal environment (Sadutto et al., 2021; Sun et al., 2021). Qingdao is a coastal tourist city with these various typical anthropogenic activities, and this is also the reason for selecting 10 different zones for collecting MPs in the present study (**Figure 1**). The differences in MP abundance (**Figure 3** and **Supplementary Figure S5**) and characteristics (**Figures 4, 5**) in the seawater and sediment from various zones clearly demonstrated that human activities greatly affected the distribution patterns of MPs in the Qingdao coastal environment. From the connection mapping between MP types, sampling zones, and shapes of the identified MPs, preliminary connections among the different characteristics and human activities were established (**Supplementary Figures S6A, B**). The characteristics of MP distribution pattern among these individual sites were various due to the complex human activities. For example, the types of MPs collected from the seawater in AF1 and AF2 were similar (**Supplementary Figure S7**), which were mainly PE and rayon fibers, indicating that the MP sources in the aquafarms were mainly from aquaculture activities such as regular stocking, feeding, harvesting, and mechanical abrasions of wave and suspended particle (Sui et al., 2020; Zhou et al., 2020). Moreover, the PVC abundance in AF1 was higher than AF2 because it was generally used in aquaculture facilities such as PVC tubes and settlement plates in the abandoned aquafarm (Bringer et al., 2021). Notably, the total abundance of MPs in the AF2 was 7.53 times lower than that of AF1, mainly due to the short-term aquaculture development and the ingestion/adhesion of the shells (Xue et al., 2020). In addition, the small neutral or negatively buoyant particles are difficult to deposit than larger ones by Stokes' law (Zwanzig, 1964), and the

large amounts of relatively small size of MPs may be transported for long distance with the current (Su et al., 2020). Furthermore, MPs could vertically transport in the water column due to biofouling and marine snow (Porter et al., 2018). In the coastal city, the harbor generally is a hotspot for MP pollution due to the frequent navigation, trade, and fishery activities (Dibke et al., 2021). In this study, the harbors are not only serviced for ships to load and unload goods (HB1, HB2) but also for reception for the disposal of waste, such as discarded fishing gear and net (HB2). The types of MPs detected in these two harbors were PE, PS, PVC, PP, PET, and PTFE, indicating that the MP sources could be plastic waste from aquaculture facilities, frequented navigation (Chen L., et al., 2021), and marine paint losses (Dibke et al., 2021). Moreover, the SDI values in the aquafarms and harbors were also higher than those of other zones in the present study, further confirming that the sources of MPs in these zones were more diverse and complex.

The MP abundance in the bathing beaches was lower than those of aquafarms and harbors (**Supplementary Figure S3A**), which was ascribed to the effective waste management strategy due to the landscape and recreation in this area of Qingdao. Even so, the extensive tourist activities in the coastal beach can be considered as potentially significant sources of plastic pollution. For example, the higher proportion of PET (14.3–14.4%) in beaches (BB1 and BB2) was mainly the result of packaging applications and clothing fibers (Ding et al., 2019). Meanwhile, the dominant fiber in BB2 (40.7–92.3%) suggested that the MP pollution may originate from the shedding of textile fabrics during recreational activities, swimming, and laundry water from the nearby hotels along the beaches (Dalla Fontana et al., 2020; Akkajit et al., 2021). Additionally, the frequently detected PS and PP in the seawater, sediment, and sand indicated that the MPs probably originated from disposable plastic containers, protective packaging, lids, bottles, and trays (Vidyasakar et al., 2018).

The MP levels in the estuary (EL) were lower in the coastal seawater but higher in the sediment than those of other zones (**Figure 3**), mainly due to the formation of heteroaggregates *via* MP with natural colloids (Wang et al., 2018; Mani et al., 2019). Additionally, previous studies pointed out that the biofouling increased the density of MP-associated particles and accelerated their sedimentation on the upstream riverbed. Similar to the estuary, the lower MP concentrations in the outlet of WWTPs in seawater are higher in sediment because not all the MPs in wastewater can be effectively removed in WWTPs. Particularly, fibers were difficult to remove in WWTPs due to their strong buoyancy (Zhang et al., 2020), thus the fiber dominated in the sewage discharge zones in the present study (33.9–57.5%, **Figure 3D**). Additionally, the proportion of MPs with high density (e.g., PET, PVC, and polyester) in the sewage discharge zones was higher than those in other zones (**Figure 4B**), resulting in settlement and accumulation of a large amount of MPs within the sediments in the sewage outlet (Margenat et al., 2021). The MP abundances and diversities were higher in all the zones stressed with human activities relative to the rural area, suggesting that human activities were the key reasons responsible for MP pollution in the Qingdao coastal environment, particularly aquaculture, navigation, and tourism.

Environmental Factors Affecting MP Pollution in Qingdao Coastal Environment

Environmental factors affecting MP pollution in coastal environments generally include wind, weather, and current conditions (Zhang et al., 2020), compared with the flow direction of the Qingdao coastal current and the residual current in Jiaozhou Bay, which was inconsistent with the MP distribution pattern of this study (**Supplemental Figure S8**). The results showed that the distribution of MPs in seawater could not conform to the flow track of the current, implying that human activities dominantly contributed to the spatial patterns of MPs in the seawater instead of the current and wind. In this study, the abundances of MPs in the sediments of Jiaozhou Bay were 2–3 orders of magnitude higher than those reported in a previous study (Zheng et al., 2019), mainly due to the locations of the sampling sites close to human anthropic zones. In addition, Van et al. (2017) found that the MP distribution was not affected by season in the Israeli Mediterranean coastal waters, although it was found that heavy winter rains could sweep substantial volumes of light matters and floats to the sea in many previous research (Jambeck et al., 2015). On the contrary, patches of floating debris were observed in all seasons due to the local wind-induced eddies (Van et al., 2017). Still, it is difficult to distinguish the specific sources of MP pollution in the different zones of Qingdao coastal environment because of many interacting factors in the process of MP migration, settlement, and accumulation, which should be considered in the future.

The MP abundance in Jiaozhou Bay was higher than that in the open sea within the same type of human activity zones (**Supplemental Figure S6B**), mainly resulted from the different hydrological conditions. Jiaozhou Bay is a semi-enclosed bay and characterized by a weak hydrodynamic environment due to the long periods of hydraulic exchange and low tide power (Carvalho et al., 2021). Hydrological conditions play important roles in the occurrence and distribution of MPs in the water environment (Mauro et al., 2017). The weak hydrodynamics in Jiaozhou Bay could also result in aggregation of MPs, which can be difficult to migrate long distances with the tide (Zhang et al., 2020). Moreover, the weak hydraulic conditions in the semi-enclosed bay would increase the levels of pollutants such as trace metals, PPCPs, and MPs (Akhbarizadeh et al., 2018; Wang et al., 2018). MPs also can play as vectors to co-transport these chemical pollutants due to adsorption. The MPs adsorbed by chemical pollutants will then be colonized by microorganisms, resulting in biofouling and accelerating sedimentation. Moreover, owing to the restriction of water exchange at the narrow bay mouth, the inputs of large amounts of MPs in coastal cities may increase the risk of accumulation and settlement for debris (Xing et al., 2017). Therefore, MP pollution in these areas may be the result of a combination of environmental accumulation and increasing contributions from anthropogenic activities.

CONCLUSIONS

This study reported the spatial patterns of MPs pollution in coastal zones with different anthropogenic activities in the Qingdao

coastal environment. The coastal seawater was less polluted with MPs compared to other domestic and global coastal regions. The levels of MP pollution in the coastal sediment and sand subjected to different human activities were higher than those in other coastal regions. The abandoned aquafarm and harbors were the hotspot for MP accumulation in the coastal surface seawater and sediment, respectively. For the coastal beach, the highest abundance of MPs was observed in the intertidal zone of the scenic beaches and in the supratidal zone of recreational beaches. Overall, the anthropogenic activities played significant roles in determining MP spatial pollution patterns in surface seawater of the coastal environment, and anthropogenic activities and hydrodynamic conditions jointly determine MP distribution in coastal sediment and sand. Still, long-term and large-scale monitoring of MP pollution in the coastal environment should be conducted in the future to ensure that effective preventive action can be taken to control MP pollution in coastal environments.

DATA AVAILABILITY STATEMENT

The original contributions presented in the study are included in the article/**Supplementary Material**. Further inquiries can be directed to the corresponding authors.

AUTHOR CONTRIBUTIONS

YDL: Investigation, Data curation, Formal analysis, Methodology, Writing-original draft. CS: Investigation, Methodology. CL: Investigation, Formal analysis. YFL: Investigation, Formal analysis. SZ: Investigation, Writing-review and editing. YYL: Formal analysis. FK: Resources, Formal analysis, Funding acquisition, Writing-review and editing. HZ: Conceptualization, Supervision, Methodology, Data curation, Formal analysis, Writing-review and editing, Funding acquisition. XL: Resources, Methodology, Writing-review and editing. LC: Methodology, Visualization. FL: Project administration, Resources, Validation. All authors contributed to the article and approved the submitted version.

FUNDING

This research was supported by the Hainan Provincial Joint Project of Sanya Yazhou Bay Science and Technology City (220LH061), National Natural Science Foundation of China (41976146), Hainan Provincial Key Research and Development Projects (ZDYF2022SHFZ018), and National Natural Science Foundation of China (42077115).

SUPPLEMENTARY MATERIAL

The Supplementary Material for this article can be found online at: <https://www.frontiersin.org/articles/10.3389/fmars.2022.916859/full#supplementary-material>

REFERENCES

- Abbasi, S., Turner, A., Hoseini, M., and Amiri, H. (2021). Microplastics in the Lut and Kavir Deserts, Iran. *Environ. Sci. Technol.* 55, 5993–6000. doi: 10.1021/acs.est.1c00615
- Akhbarizadeh, R., Moore, F., and Keshavarzi, B. (2018). Investigating a Probable Relationship Between Microplastics and Potentially Toxic Elements in Fish Muscles From Northeast of Persian Gulf. *Environ. Pollut.* 232, 154–163. doi: 10.1016/j.envpol.2017.09.028
- Akhbarizadeh, R., Moore, F., Keshavarzi, B., and Moeinpour, A. (2017). Microplastics and Potentially Toxic Elements in Coastal Sediments of Iran's Main Oil Terminal (Khark Island). *Environ. Pollut.* 220, 720–731. doi: 10.1016/j.envpol.2016.10.038
- Akkajit, P., Tipmanee, D., Cherdasukjai, P., Suteerasak, T., and Thongnonghin, S. (2021). Occurrence and Distribution of Microplastics in Beach Sediments Along Phuket Coastline. *Mar. Pollut. Bull.* 169, 112496. doi: 10.1016/j.marpolbul.2021.112496
- Bagaev, A., Khatmullina, L., and Chubarenko, I. (2018). Anthropogenic Microlitter in the Baltic Sea Water Column. *Mar. Pollut. Bull.* 129, 918–923. doi: 10.1016/j.marpolbul.2017.10.049
- Bai, Y., Wu, B., Chen, W., Li, M., and Weng, Y. (2022). Influences of Energetic Typhoons on the Redistributions of Heavy Metals in Sediments Along the Leizhou Peninsula Coast, Southern China. *Mar. Pollut. Bull.* 174, 113268. doi: 10.1016/j.marpolbul.2021.113268
- Bie, S., Yang, L., Zhang, Y., Huang, Q., Li, J., Zhao, T., et al. (2021). Source Appointment of PM_{2.5} in Qingdao Port, East of China. *Sci. Tot. Environ.* 755, 142456. doi: 10.1016/j.scitotenv.2020.142456
- Brignac, K. C., Jung, M. R., King, C., Royer, S., and Lynch, J. M. (2019). Marine Debris Polymers on Main Hawaiian Island Beaches, Sea Surface, and Seafloor. *Environ. Sci. Technol.* 53, 12218–12226. doi: 10.1021/acs.est.9b03561
- Bringer, A., Floch, S.L., Kerstan, A., and Thomas, H. (2021). Coastal Ecosystem Inventory With Characterization and Identification of Plastic Contamination and Additives From Aquaculture Materials. *Mar. Pollut. Bull.* 167, 112286. doi: 10.1016/j.marpolbul.2021.112286
- Cai, M., He, H., Liu, M., Li, S., Tang, G., Wang, W., et al. (2018). Lost But Can't be Neglected: Huge Quantities of Small Microplastics Hide in the South China Sea. *Sci. Tot. Environ.* 15, 1206–1216. doi: 10.1016/j.scitotenv.2018.03.197
- Cao, Y., Xin, M., Wang, B., Lin, C., Liu, X., He, M., et al. (2020). Spatiotemporal Distribution, Source, and Ecological Risk of Polycyclic Aromatic Hydrocarbons (PAHs) in the Urbanized Semi-Enclosed Jiaozhou Bay, China. *Sci. Tot. Environ.* 717, 137224. doi: 10.1016/j.scitotenv.2020.137224
- Carretero, O., Gago, J., and Viñas, L. (2020). From the Coast to the Shelf: Microplastics in Rias Baixas and Mio River Shelf Sediments (NW Spain). *Mar. Pollut. Bull.* 162, 111814. doi: 10.1016/j.marpolbul.2020.111814
- Carvalho, A., Garcia, F., Riem-Galliano, L., Tudesque, L., and Cucherousset, J. (2021). Urbanization and Hydrological Conditions Drive the Spatial and Temporal Variability of Microplastic Pollution in the Garonne River. *Sci. Tot. Environ.* 769, 144479. doi: 10.1016/j.scitotenv.2020.144479
- Castro, R. O., Silva, M., Marques, M., and Araújo, F. V. D. (2020). Spatio-temporal Evaluation of Macro, Meso and Microplastics in Surface Waters, Bottom and Beach Sediments of Two Embayments in Niterói, RJ, Brazil. *Mar. Pollut. Bull.* 160, 111537. doi: 10.1016/j.marpolbul.2020.111537
- Chae, Y., and An, Y. J. (2017). Effects of Micro- and Nanoplastics on Aquatic Ecosystems: Current Research Trends and Perspectives. *Mar. Pollut. Bull.* 124, 624–632. doi: 10.1016/j.marpolbul.2017.01.070
- Chen, X., Chen, X., Zhao, Y., Zhou, H., Xiong, X., and Wu, C. (2020). Effects of Microplastic Biofilms on Nutrient Cycling in Simulated Freshwater Systems. *Sci. Tot. Environ.* 719, 137271–137276. doi: 10.1016/j.scitotenv.2020.137276
- Chen, C. F., Ju, Y. R., Lim, Y. C., Chen, C. W., and Dong, C. D. (2021). Seasonal Variation of Diversity, Weathering, and Inventory of Microplastics in Coast and Harbor Sediments. *Sci. Tot. Environ.* 781, 146610. doi: 10.1016/j.scitotenv.2021.146610
- Chen, L., Li, J., Tang, Y., Wang, S., Lu, X., Cheng, Z., et al. (2021). Typhoon-Induced Turbulence Redistributed Microplastics in Coastal Areas and Reformed Plasticsphere Community. *Wat. Res.* 204, 117580. doi: 10.1016/j.watres.2021.117580
- Cordova, M. R., Purwiyanto, A., and Suteja, Y. (2019). Abundance and Characteristics of Microplastics in the Northern Coastal Waters of Surabaya, Indonesia. *Mar. Pollut. Bull.* 142, 183–188. doi: 10.1016/j.marpolbul.2019.03.040
- Cózar, A., Echevarría, F., Gonzálezgordillo, J. I., Irigoien, X., Úbeda, B., Hernández, S., et al. (2014). Plastic Debris in the Open Ocean. *Proc. Natl. Acad. Sci. U.S.A.* 111, 10239–10244. doi: 10.1073/pnas.1314705111
- Dalla Fontana, G.D., Mossotti, R., and Montarsolo, A. (2020). Assessment of Microplastics Release from Polyester Fabrics: The Impact of Different Washing Conditions. *Environ. Pollut.* 264, 113960. doi: 10.1016/j.envpol.2020.113960
- Dibke, C., Fischer, M., and Scholz-Bottcher, B. M. (2021). Microplastic Mass Concentrations and Distribution in German Bight Waters by Pyrolysis–Gas Chromatography–Mass Spectrometry/Thermochemolysis Reveal Potential Impact of Marine Coatings: Do Ships Leave Skid Marks? *Environ. Sci. Technol.* 55, 2285–2295. doi: 10.1021/acs.est.0c04522
- Ding, J., Jiang, F., Li, J., Wang, Z., Sun, C., Wang, Z., et al. (2019). Microplastics in the Coral Reef Systems From Xisha Islands of South China Sea. *Environ. Sci. Technol.* 53, 8036–8046. doi: 10.1021/acs.est.9b01452
- Dong, M., Zhang, Q., Xing, X., Chen, W., She, Z., and Luo, Z. (2020). Raman Spectra and Surface Changes of Microplastics Weathered Under Natural Environments. *Sci. Tot. Environ.* 739, 139990. doi: 10.1016/j.scitotenv.2020.139990
- Dowarah, K., and Devipriya, S. P. (2019). Microplastic Prevalence in the Beaches of Puducherry, India and its Correlation With Fishing and Tourism/Recreational Activities. *Mar. Pollut. Bull.* 148, 123–133. doi: 10.1016/j.marpolbul.2019.07.066
- Duan, Z., Duan, X., Zhao, S., Wang, X., and Wang, L. (2020). Barrier Function of Zebrafish Embryonic Chorions Against Microplastics and Nanoplastics and its Impact on Embryo Development. *J. Haz. Mater.* 395, 122621. doi: 10.1016/j.jhazmat.2020.122621
- EO, S., Hong, S. H., Song, Y. K., Lee, J., Lee, J., and Shim, W. J. (2018). Abundance, Composition, and Distribution of Microplastics Larger Than 20 μm in Sand Beaches of South Korea. *Environ. Pollut.* 238, 894–902. doi: 10.1016/j.envpol.2018.03.096
- Fok, L., Cheung, P., Tang, T., and Li, W. (2017). Size Distribution of Stranded Small Plastic Debris on the Coast of Guangdong, South China. *Environ. Pollut.* 220, 407–412. doi: 10.1016/j.envpol.2016.09.079
- Frere, L., Paul, I., Rinnert, E., Petton, S., Jaffré, J., Bihannic, I., et al. (2017). Influence of Environmental and Anthropogenic Factors on the Composition, Concentration and Spatial Distribution of Microplastics: A Case Study of the Bay of Brest (Brittany, France). *Environ. Pollut.* 225, 211–222. doi: 10.1016/j.envpol.2017.03.023
- Fu, J., Fu, K., Chen, Y., Li, X., and Fu, J. (2021). Long-range Transport, Trophic Transfer, and Ecological Risks of Organophosphate Esters in Remote Areas. *Environ. Sci. Technol.* 55, 10192–10209. doi: 10.1021/acs.est.0c08822
- Gao, F., Li, J., Hu, J., Sui, B., and Ju, P. (2021). The Seasonal Distribution Characteristics of Microplastics on Bathing Beaches Along the Coast of Qingdao, China. *Sci. Tot. Environ.* 783, 146969. doi: 10.1016/j.scitotenv.2021.146969
- Gardona, T., Morvana, L., Huvet, A., Quillien, V., Soyez, C., Moullac, G. L., et al. (2020). Microplastics Induce Dose-Specific Transcriptomic Disruptions in Energy Metabolism and Immunity of the Pearl Oyster *Pinctada Margaritifera*. *Environ. Pollut.* 266, 115180. doi: 10.1016/j.envpol.2020.115180
- Gaylard, S., Waycott, M., and Lavery, P. (2020). Review of Coast and Marine Ecosystems in Temperate Australia Demonstrates a Wealth of Ecosystem Services. *Front. Mar. Sci.* 7, 00453. doi: 10.3389/fmars.2020.00453
- Geyer, R., Jambeck, J. R., and Law, K. L. (2017). Production, Use, and Fate of All Plastics Ever Made. *Sci. Adv.* 3, e1700782. doi: 10.1126/sciadv.1700782
- Gupta, P., Saha, M., Rathore, C., and Suneel, V. (2021). Spatial and Seasonal Variation of Microplastics and Possible Sources in the Estuarine System From Central West Coast of India. *Environ. Pollut.* 288, 117665. doi: 10.1016/j.envpol.2021.117665
- Hal, N., Ariel, A., and Angel, D. L. (2017). Exceptionally High Abundances of Microplastics in the Oligotrophic Israeli Mediterranean Coastal Waters. *Mar. Pollut. Bull.* 116, 151–155. doi: 10.1016/j.marpolbul.2016.12.052
- Hartmann, N., Hüffer, T., Thompson, R. C., Hassellöv, M., Verschoor, A., Daugaard, A. E., et al. (2019). Are We Speaking the Same Language? Recommendations for a Definition and Categorization Framework for Plastic Debris. *Environ. Sci. Technol.* 53, 4678–4679. doi: 10.1021/acs.est.9b02238
- Hengstmann, E., Tamminga, M., Bruch, C. V., and Fischer, E. K. (2018). Microplastic in Beach Sediments of the Isle of Rugen (Baltic Sea)—implementing a Novel Glass Elutriation Column. *Mar. Pollut. Bull.* 126, 263–274. doi: 10.1016/j.marpolbul.2017.11.010
- Jambeck, J. R., Geyer, R., Wilcox, C., Siegler, T. R., Perryman, M., Andrady, A., et al. (2015). Plastic Waste Inputs From Land Into the Ocean. *Science* 347, 768–771. doi: 10.1126/science.1260352

- Jebara, A., Turco, V. L., Potorti, A. G., Bartolomeo, G., and Bella, G. D. (2020). Organic Pollutants in Marine Samples From Tunisian Coast: Occurrence and Associated Human Health Risks. *Environ. Pollut.* 271, 116266. doi: 10.1016/j.envpol.2020.116266
- Jorquera, A., Castillo, C., Murillo, V., Araya, J., Pinochet, J., Narváez, D., et al. (2022). Physical and Anthropogenic Drivers Shaping the Spatial Distribution of Microplastics in the Marine Sediments of Chilean Fjords. *Sci. Tot. Environ.* 814, 152506. doi: 10.1016/j.scitotenv.2021.152506
- Jung, J. W., Park, J. W., Eo, S., Choi, J., Song, Y. K., Cho, Y., et al. (2020). Ecological Risk Assessment of Microplastics in Coastal, Shelf, and Deep Sea Waters With a Consideration of Environmentally Relevant Size and Shape. *Environ. Pollut.* 270, 116217. doi: 10.1016/j.envpol.2020.116217
- Kang, H. M., Byeon, E., Jeong, H., Kim, M. S., and Lee, J. S. (2020). Different Effects of Nano- and Microplastics on Oxidative Status and Gut Microbiota in the Marine Medaka *Oryzias Melastigma*. *J. Haz. Mater.* 404, 124207. doi: 10.1016/j.jhazmat.2020.124207
- Lastra, M., Lopez, J., and Neves, G. (2015). Algal Decay, Temperature and Body Size Influencing Trophic Behaviour of Wrack Consumers in Sandy Beaches. *Mar. Biol.* 162, 221–233. doi: 10.1007/s00227-014-2562-z
- Lau, W. W. Y., Shiran, Y., Bailey, R. M., Cook, E., Stuchtey, M. R., Koskella, J., et al. (2020). Evaluating Scenarios Toward Zero Plastic Pollution. *Science* 369, 1455–1461. doi: 10.1126/science.aba9475
- Lenaker, P. L., Baldwin, A. K., Corsi, S. R., Mason, S. A., Reneau, P. C., and Scott, J. W. (2019). Vertical Distribution of Microplastics in the Water Column and Surficial Sediment From the Milwaukee River Basin to Lake Michigan. *Environ. Sci. Technol.* 53, 12227–12237. doi: 10.1021/acs.est.9b03850
- Leslie, H. A., Brandsma, S. H., Velzen, M. J. M., and Vethaak, A. D. (2017). Microplastics en route: Field Measurements in the Dutch River Delta and Amsterdam Canals, Wastewater Treatment Plants, North Sea Sediments and Biota. *Environ. Int.* 101, 133–42. doi: 10.1016/j.envint.2017.01.018
- Li, C., Gan, Y., Zhang, C., He, H., Fang, J., Wang, L., et al. (2020). "Microplastic Communities" in Different Environments: Differences, Links, and Role of Diversity Index in Source Analysis. *Wat. Res.* 188, 116574. doi: 10.1016/j.watres.2020.116574
- Li, M., Chen, D., Liu, Y., Chuang, C. Y., Kong, F., Harrison, P. J., et al. (2018). Exposure of Engineered Nanoparticles to *Alexandrium tamarense* (Dinophyceae): Healthy Impacts of Nanoparticles Via Toxin-Producing Dinoflagellate. *Sci. Tot. Environ.* 610–1, 356–66. doi: 10.1016/j.scitotenv.2017.05.170
- Lindeque, P. K., Cole, M., Coppock, R. L., Lewis, C. N., Miller, R. Z., Watts, A. J. R., et al. (2020). Are We Underestimating Microplastic Abundance in the Marine Environment? A Comparison of Microplastic Capture With Nets of Different Mesh-Size. *Environ. Pollut.* 265, 114721. doi: 10.1016/j.envpol.2020.114721
- Liu, Y., Zhang, J., Tang, Y., He, Y., Li, Y., You, J., et al. (2021). Effects of Anthropogenic Discharge and Hydraulic Deposition on the Distribution and Accumulation of Microplastics in Surface Sediments of a Typical Seagoing River: The Haihe River. *J. Haz. Mater.* 404, 124180. doi: 10.1016/j.jhazmat.2020.124180
- Liu, T., Zhao, Y., Zhu, M., Liang, J., Zheng, S., and Sun, X. (2020). Seasonal Variation of Micro- and Meso-Plastics in the Seawater of Jiaozhou Bay, the Yellow Sea. *Mar. Pollut. Bull.* 152, 110922. doi: 10.1016/j.marpolbul.2020.110922
- Liu, L., Zheng, H., Luan, L., Luo, X., Wang, X., Lu, H., et al. (2021). Functionalized Polystyrene Nanoplastic-Induced Energy Homeostasis Imbalance and the Immunomodulation Dysfunction of Marine Clams (*Meretrix Meretrix*) at Environmentally Relevant Concentrations. *Environ. Sci. Nano.* 8, 2030–2048. doi: 10.1039/D1EN00212K
- Li, R., Zhang, L., Xue, B., and Wang, Y. (2019). Abundance and Characteristics of Microplastics in the Mangrove Sediment of the Semi-Enclosed Maowei Sea of the South China Sea: New Implications for Location, Rhizosphere, and Sediment Compositions. *Environ. Pollut.* 244, 685–692. doi: 10.1016/j.envpol.2018.10.089
- Luo, Y. (2016). Sustainability Associated Coastal Eco-Environmental Problems and Coastal Science Development in China. *Bull. Chin. Acad. Sci.* 31, 1133–42. doi: 10.16418/j.issn.1000-3045.2016.10.001
- MacLeod, M., Arp, H. P. H., Tekman, M. B., and Jahnke, A. (2021). The Global Threat From Plastic Pollution. *Science* 373, 61–65. doi: 10.1126/science.aba5433
- Mani, T., Primpke, S., Lorenz, C., Gerdt, G., and Burkhardt-holm, P. (2019). Microplastic Pollution in Benthic Mid-Stream Sediments of the Rhine River. *Environ. Sci. Technol.* 21, 6053–6062. doi: 10.1021/acs.est.9b01363
- Margenat, H., Nel, H. A., and Stonedahl, S. H. (2021). Hydrologic Controls on the Accumulation of Different Sized Microplastics in the Streambed Sediments Downstream of a Wastewater Treatment Plant (Catalonia, Spain). *Environ. Res. Lett.* 11, 115012. doi: 10.1088/1748-9326/ac3179
- Masura, J., Baker, J., Foster, G., and Arthur, C. (2015). *Laboratory Methods for the Analysis of Microplastics in the Marine Environment* (NOAA Technical Memorandum NOS-OR&R-48). Available online at: https://marinedebris.noaa.gov/sites/default/files/publications-files/noaa_microplastics_methods_manual.pdf.
- Matsuguma, Y., Takada, H., Kumata, H., Herring, C., Editor, T., and Arthur, C. (2017). Microplastics in Sediment Cores From Asia and Africa as Indicators of Temporal Trends in Plastic Pollution. *Arch. Environ. Contam. Toxicol.* 73, 230–239. doi: 10.1007/s00244-017-0414-9
- Mauro, R. D., Kupchik, M. J., and Benfield, M. C. (2017). Abundant Plankton-Sized Microplastic Particles in Shelf Waters of the Northern Gulf of Mexico. *Environ. Pollut.* 230, 798–809. doi: 10.1016/j.envpol.2017.07.030
- Meng, Y., Kelly, F. J., and Wright, S. L. (2020). Advances and Challenges of Microplastic Pollution in Freshwater Ecosystems: A UK Perspective. *Environ. Pollut.* 256, 113441–113445. doi: 10.1016/j.envpol.2019.113445
- Nel, H. A., and Froneman, P. W. (2015). A Quantitative Analysis of Microplastic Pollution Along the South-Eastern Coastline of South Africa. *Mar. Pollut. Bull.* 101, 274–279. doi: 10.1016/j.marpolbul.2015.09.043
- Nelms, S. E., Parry, H. E., Bennett, K. A., Galloway, T. S., Godley, B. J., Santillo, D., et al. (2019). What Goes in, Must Come Out: Combining Scat-Based Molecular Diet Analysis and Quantification of Ingested Microplastics in a Marine Top Predator. *Methods Ecol. Evol.* 10, 1712–1722. doi: 10.1111/2041-210X.13271
- Oliveira, J. P. J., Estrela, F. N., Rodrigues, A. S. D. L., Guimaraes, A. T. B., Rocha, T. L., and Malafaia, G. (2021). Behavioral and Biochemical Consequences of *Danio Rerio* Larvae Exposure to Polylactic Acid Bioplastic. *J. Haz. Mater.* 404, 124152. doi: 10.1016/j.jhazmat.2020.124152
- Park, H., Oh, M. J., Kim, P. G., Kim, G., and Kwon, J. H. (2020). National Reconnaissance Survey of Microplastics in Municipal Wastewater Treatment Plants in Korea. *Environ. Sci. Technol.* 54, 1503–1512. doi: 10.1021/acs.est.9b04929
- Patchaiyappan, A. K., Ahmed, S. Z., Dowarah, K., Khadanga, S. S., and Devipriya, S. P. (2021). Prevalence of Microplastics in the Sediments of Odisha Beaches, Southeastern Coast of India. *Mar. Pollut. Bull.* 167, 1503–1512. doi: 10.1016/j.marpolbul.2021.112265
- Peller, J., Nevers, M. B., Byappanahalli, M., Nelson, C., and Shidler, S. (2021). Sequestration of Microfibers and Other Microplastics by Green Algae, Cladophora, in the US Great Lakes. *Environ. Pollut.* 276, 116695. doi: 10.1016/j.envpol.2021.116695
- Peng, L., Fu, D., Qi, H., Lan, C. Q., Yu, H., and Ge, C. (2020). Micro- and Nano-Plastics in Marine Environment: Source, Distribution and Threats—a Review. *Sci. Tot. Environ.* 698, 134251–134254. doi: 10.1016/j.scitotenv.2019.134254
- Pervez, R., Wang, Y., Mahmood, Q., Zahir, M., and Jattak, Z. (2020). Abundance, Type, and Origin of Litter on No. 1 Bathing Beach of Qingdao, China. *J. Coast. Conserv.* 24, s11852. doi: 10.1007/s11852-020-00751-x
- Pintado-Herrera, M. G., Allan, I. J., Gonzalez-Mazo, E., and Lara-Martin, P. A. (2020). Passive Samplers vs Sentinel Organisms: One-Year Monitoring of Priority and Emerging Contaminants in Coastal Waters. *Environ. Sci. Technol.* 54, 6693–6702. doi: 10.1021/acs.est.0c00522
- Plastics Europe (2021). *Production and Prices of Plastics Continued to Rise in the Final Quarter 2021*, 8 pp. Available online at: <https://plasticseurope.org/wp-content/uploads/2022/03/Quarterly-Report-Q4-2021.pdf> (assessed April 24, 2022).
- Porter, A., Lyons, B. P., Galloway, T. S., and Lewis, C. (2018). Role of Marine Snows in Microplastic Fate and Bioavailability. *Environ. Sci. Technol.* 52, 7111–9. doi: 10.1021/acs.est.8b01000
- Prata, J. C., Da Costa, J. P., Duarte, A. C., and Rocha-Santos, T. (2019). Methods for Sampling and Detection of Microplastics in Water and Sediment: A Critical Review. *Trend. Analyt. Chem.* 110, 150–159. doi: 10.1016/j.trac.2018.10.029
- Preston, W. F., Silburn, B., Meakins, B., Herring, C., Editor, T., and Arthur, C. (2021). Meso- and Microplastics Monitoring in Harbour Environments: A Case Study for the Port of Durban, South Africa. *Mar. Pollut. Bull.* 163, 4836. doi: 10.1016/j.marpolbul.2020.111948
- Qiu, Q., Peng, J., Yu, X., Chen, F., Wang, J., and Dong, F. (2015). Occurrence of Microplastics in the Coastal Marine Environment: First Observation on Sediment of China. *Mar. Pollut. Bull.* 98, 274–280. doi: 10.1016/j.marpolbul.2015.07.028

- Rochman, C. M., and Hoellein, T. (2020). The Global Odyssey of Plastic Pollution. *Science* 368, 1184–1185. doi: 10.1126/science.abc4428
- Sadutto, D., Andreu, V., Ilo, T., Akkanen, J., and Pico, Y. (2021). Pharmaceuticals and Personal Care Products in a Mediterranean Coastal Wetland: Impact of Anthropogenic and Spatial Factors and Environmental Risk Assessment. *Environ. Pollut.* 271, 116353. doi: 10.1016/j.envpol.2020.116353
- Santos, R. G., Machovsky-Capuska, G. E., and Andrades, R. (2021). Plastic Ingestion as an Evolutionary Trap: Toward a Holistic Understanding. *Science* 373, 56–60. doi: 10.1126/science.abh0945
- Sathish, M. N., Jeyasanta, K. I., and Patterson, J. (2020). Monitoring of Microplastics in the Clam *Donax Cuneatus* and Its Habitat in Tuticorin Coast of Gulf of Mannar (GoM), India. *Environ. Pollut.* 266, 115219. doi: 10.1016/j.envpol.2020.115219
- Sui, Q., Zhang, L., Xia, B., Chen, B., Sun, X., Zhu, L., et al. (2020). Spatiotemporal Distribution, Source Identification and Inventory of Microplastics in Surface Sediments From Sanggou Bay, China. *Sci. Tot. Environ.* 723, 138064. doi: 10.1016/j.scitotenv.2020.138064
- Sun, X., Wang, T., Chen, B., Booth, A. M., and Xia, B. (2021). Factors Influencing the Occurrence and Distribution of Microplastics in Coastal Sediments: From Source to Sink. *J. Haz. Mater.* 410, 124982. doi: 10.1016/j.jhazmat.2020.124982
- Su, L., Sharp, S. M., Pettigrove, V. J., Craig, N., Nan, B., Du, F., et al. (2020). Superimposed Microplastic Pollution in a Coastal Metropolis. *Wat. Res.* 168, 115140. doi: 10.1016/j.watres.2019.115140
- Tang, G., Liu, M., Zhou, Q., He, H., Chen, K., and Zhang, H. (2018). Microplastics and Polycyclic Aromatic Hydrocarbons (PAHs) in Xiamen Coastal Areas: Implications for Anthropogenic Impacts. *Sci. Tot. Environ.* 634, 811–820. doi: 10.1016/j.scitotenv.2018.03.336
- Thomas, M., Meulen, M., Devriese, L. I., Leslie, H. A., Huvet, A., and Frère, L. (2017). Microplastics Baseline Surveys at the Water Surface and in Sediments of the North–East Atlantic. *Front. Mar. Sci.* 4, 135. doi: 10.3389/fmars.2017.00135
- Tiwari, M., Rathod, T. D., Ajmal, P. Y., Bhargare, R. C., and Sahu, S. K. (2019). Distribution and Characterization of Microplastics in Beach Sand From Three Different Indian Coastal Environments. *Mar. Pollut. Bull.* 140, 262–273. doi: 10.1016/j.marpolbul.2019.01.055
- Trestrail, C., Walpitagama, M., Miranda, A., Nugegoda, D., and Shimeta, J. (2021). Microplastics Alter Digestive Enzyme Activities in the Marine Bivalve, *Mytilus Galloprovincialis*. *Sci. Tot. Environ.* 779, 146418. doi: 10.1016/j.scitotenv.2021.146418
- Tu, H. M., Fan, M. W., and Ko, C. J. (2020). Different Habitat Types Affect Bird Richness and Evenness. *Sci. Rep.* 10, 1221. doi: 10.1038/s41598-020-58202-4
- Van, D.H.N., Ariel, A., and Angel, D.L. (2017). Exceptionally High Abundances of Microplastics in the Oligotrophic Israeli Mediterranean Coastal Waters. *Mar. Pollut. Bull.* 116, 151–5. doi: 10.1016/j.marpolbul.2016.12.052
- Vidyasakar, A., Neelavannan, K., Krishnakumar, S., Prabakaran, G., Priyanka, S. A., Magesh, N. S., et al. (2018). Macrodebris and Microplastic Distribution in the Beaches of Rameswaram Coral Island, Gulf of Mannar, Southeast Coast of India: A First Report. *Mar. Pollut. Bull.* 137, 610–616. doi: 10.1016/j.marpolbul.2018.11.007
- Wang, X., Liu, L., Zheng, H., Wang, M., Fu, Y., Luo, X., et al. (2020b). Polystyrene Microplastics Impaired the Feeding and Swimming Behavior of Mysid Shrimp *Neomysis Japonica*. *Mar. Polluti. Bull.* 150, 110660. doi: 10.1016/j.marpolbul.2019.110660
- Wang, S., Xue, N., Li, W., Zhang, D., and Luo, Y. (2019). Selectively Enrichment of Antibiotics and ARGs by Microplastics in River, Estuary and Marine Waters. *Sci. Tot. Environ.* 708, 134594. doi: 10.1016/j.scitotenv.2019.134594
- Wang, X., Zheng, H., Zhao, J., Luo, X., and Xing, B. (2020a). Photodegradation Elevated the Toxicity of Polystyrene Microplastics to Grouper (*Epinephelus Moara*) Through Disrupting Hepatic Lipid Homeostasis. *Environ. Sci. Technol.* 54, 6202–6212. doi: 10.1021/acs.est.9b07016
- Wang, T., Zou, X., Li, B., Yao, Y., Li, J., Hui, H., et al. (2018). Microplastics in a Wind Farm Area: A Case Study at the Rudong Offshore Wind Farm, Yellow Sea, China. *Mar. Pollut. Bull.* 128, 466–474. doi: 10.1016/j.marpolbul.2018.01.050
- Watkins, L., Sullivan, P. J., and Walter, M. T. (2021). What You Net Depends on If You Grab: A Meta-Analysis of Sampling Method's Impact on Measured Aquatic Microplastic Concentration. *Environ. Sci. Technol.* 55, 12930–12942. doi: 10.1021/acs.est.1c03019
- Xie, H., Chen, J., Feng, L., He, L., Zhou, C., Hong, P., et al. (2021). Chemotaxis-selective Colonization of Mangrove Rhizosphere Microbes on Nine Different Microplastics. *Sci. Tot. Environ.* 752, 142223. doi: 10.1016/j.scitotenv.2020.142223
- Xing, J., Song, J., Yuan, H., Li, X., Li, N., Duan, L., et al. (2017). Fluxes, Seasonal Patterns and Sources of Various Nutrient Species (Nitrogen, Phosphorus and Silicon) in Atmospheric Wet Deposition and Their Ecological Effects on Jiaozhou Bay, North China. *Sci. Tot. Environ.* 576, 617–627. doi: 10.1016/j.scitotenv.2016.10.134
- Xiong, X., Hu, X., Guo, Y., Yu, L., Chen, L., and Xue, Y. (2019). Existence, morphology and structure of the Yellow Sea Warm Current Branch approaching waters offshore Qingdao, China. *Sci. China. Earth. Sci.* 62, 1167–1180. doi: 10.1007/s11430-018-9331-1
- Xu, S., Chen, L., Zhang, K., Cao, Y., Ma, Y., Chau, H. S., et al. (2022). Microplastic Occurrence in the Northern South China Sea, a Case for Pre and Post Cyclone Analysis. *Chemosphere* 296, 133980. doi: 10.1016/j.chemosphere.2022.133980
- Xue, B., Zhang, L., Li, R., Wang, Y., and Wang, S. (2020). Underestimated Microplastic Pollution Derived From Fishery Activities and "Hidden" in Deep Sediment. *Environ. Sci. Technol.* 54, 2210–2217. doi: 10.1021/acs.est.9b04850
- Zhang, T., Wang, J., Liu, D., Sun, Z., Tang, R., Ma, X., et al. (2022). Loading of Microplastics by Two Related Macroalgae in a Sea Area Where Gold and Green Tides Occur Simultaneously. *Sci. Tot. Environ.* 814, 152809. doi: 10.1016/j.scitotenv.2021.152809
- Zhang, L., Zhang, S., Guo, J., Yu, K., Wang, Y., and Li, R. (2020). Dynamic Distribution of Microplastics in Mangrove Sediments in Beibu Gulf, South China: Implications of Tidal Current Velocity and Tidal Range. *J. Haz. Mater.* 399, 122849. doi: 10.1016/j.jhazmat.2020.122849
- Zhao, S., Ward, J. E., Danley, M., and Mincer, T. (2018). Field-based Evidence for Trophic Transfer. *Environ. Sci. Technol.* 52, 11038–11048. doi: 10.1021/acs.est.8b03467
- Zhao, J., Wen, R., Tang, J., Liu, Y., Yin, X., Cao, R., et al. (2018). Microplastic Pollution in Sediments From the Bohai Sea and the Yellow Sea, China. *Sci. Tot. Environ.* 640, 637–645. doi: 10.1016/j.scitotenv.2018.05.346
- Zheng, Y., Li, J., Cao, W., Liu, X., Jiang, F., Ding, J., et al. (2019). Distribution Characteristics of Microplastics in the Seawater and Sediment: A Case Study in Jiaozhou Bay, China. *Sci. Tot. Environ.* 674, 27–35. doi: 10.1016/j.scitotenv.2019.04.008
- Zheng, Z., Wu, Z., Chen, Y., Yang, Z., and Marinello, F. (2020). Exploration of Eco-Environment and Urbanization Changes in Coastal Zones: A Case Study in China Over the Past 20 Years. *Ecol. Indic.* 119, 106847. doi: 10.1016/j.ecolind.2020.106847
- Zhou, Q., Zhang, H., Waniek, J. J., and Luo, Y. (2020). *The Distribution and Characteristics of Microplastics in Coastal Beaches and Mangrove Wetlands, Microplastics in Terrestrial Environments*. 77–92 Switzerland: Springer Nature Switzerland AG.
- Zhu, L., Bai, H., Chen, B., Sun, X., Qu, K., and Xia, B. (2018). Microplastic Pollution in North Yellow Sea, China: Observations on Occurrence, Distribution and Identification. *Sci. Tot. Environ.* 636, 20–29. doi: 10.1016/j.scitotenv.2018.04.182
- Zhu, J., Zhang, Q., Li, Y., Tan, S., Kang, Z., Yu, X., et al. (2019). Microplastic Pollution in the Maowei Sea, A Typical Mariculture Bay of China. *Sci. Tot. Environ.* 658, 62–68. doi: 10.1016/j.scitotenv.2018.12.192
- Zwanzig, R. (1964). Hydrodynamic Fluctuations and Stokes' Law Friction. *J. Res. Natl. Inst. Stand. Technol.* 68, 143–145. doi: 10.6028/jres.068B.019

Conflict of Interest: The authors declare that the research was conducted in the absence of any commercial or financial relationships that could be construed as a potential conflict of interest.

Publisher's Note: All claims expressed in this article are solely those of the authors and do not necessarily represent those of their affiliated organizations, or those of the publisher, the editors and the reviewers. Any product that may be evaluated in this article, or claim that may be made by its manufacturer, is not guaranteed or endorsed by the publisher.

Copyright © 2022 Luo, Sun, Li, Liu, Zhao, Li, Kong, Zheng, Luo, Chen and Li. This is an open-access article distributed under the terms of the Creative Commons Attribution License (CC BY). The use, distribution or reproduction in other forums is permitted, provided the original author(s) and the copyright owner(s) are credited and that the original publication in this journal is cited, in accordance with accepted academic practice. No use, distribution or reproduction is permitted which does not comply with these terms.